OPTIMIZATION AND FABRICATION OF DISSOLVABLE MICRONEEDLE ARRAYS FOR GLUCOSAMINE, CHONDROITIN, AND HYALURONIC ACID FOR OSTEOARTHRITIS TREATMENT

by
ANDISHEH CHOUPANI

Submitted to the Graduate School of Engineering and Natural Sciences
in partial fulfilment of
the requirements for the degree of
Master of Science

Sabancı University
July 2022

OPTIMIZATION AND FABRICATION OF DISSOLVABLE MICRONEEDLE ARRAYS FOR GLUCOSAMINE, CHONDROITIN, AND HYALURONIC ACID FOR OSTEOARTHRITIS TREATMENT

Approved by:

Assist. Prof. Dr. Bekir Bediz .....
(Thesis Supervisor)

Assoc. Prof. Dr. Feray Bakan .....

Prof. Dr. Feza Korkusuz .....

Date of Approval: .....

Abstract

OPTIMIZATION AND FABRICATION OF DISSOLVABLE MICRONEEDLE ARRAYS FOR GLUCOSAMINE, CHONDROITIN, AND HYALURONIC ACID FOR OSTEOARTHRITIS TREATMENT

Andisheh Choupani

Mechatronics Engineering, Master's Thesis, July 2022

Thesis Supervisor: Assist. Prof. Bekir Bediz

Keywords: drug delivery, microneedle, microneedle array, micro-manufacturing, structural optimization, finite element analysis, osteoarthritis.

Due to their various advantages compared to conventional drug delivery systems such as hypodermic injections and oral medications, microneedle arrays (MNAs) is a promising drug delivery system. Needle geometry is an important parameter to achieve enhanced performance of the MNA. Thus, it is crucial to develop numerical models and optimize the needle geometry. In this work, a multi-objective optimization framework is presented to determine the optimum design of MNAs. For this purpose, a three-dimensional model of a single microneedle (MN) is developed. To simulate the insertion process, a load is applied at the tip region. Since depending on the orientation of the force, the failure can be either due to the buckling or bending, a multi-objective optimization based on non-dominated sorting genetic algorithm II (NSGA-II) is performed to obtain geometrical properties such as needle width, tip (apex) angle, base fillet radius. The objective is to prevent mechanical failure when the needles are inserted into the skin; thus the objective function is set to minimize the maximum stress occurring throughout the structure. As a result, the chosen dimensions provides a safety factor of 8.8. Based on the optimized geometry of the needles, master molds for MNAs are then fabricated from PMMA using mechanical micromachining process. This fabrication method is selected mainly due to the geometry capability, production speed, production cost, and the variety of materials that can be used. These fabricated master molds are used repeatedly to fabricate Polydimethylsiloxane (PDMS) production (female) molds through micro-

molding approach. In this study, the materials utilized in fabrication of MNAs are mainly considered for the application purpose of Osteoarthritis (OA), which is a degenerative chronic disorder, not only affecting the articular cartilage, but also the subchondral bone, synovium, joint capsule, and soft tissues around the joint. The main purpose of OA treatment is to preserve the structure and functions of the joint, reduce inflammation and fibrosis, and prevent progressive cartilage loss. Medical support therapies including glucosaminoglycan (GAG), chondroitin (CS), and hyaluronic acid (HA), are among the regenerative strategies to prevent surgical joint replacement. However, they must be taken orally in high doses, continuously and for weeks to months causing series of side effects in the gastrointestinal system. Therefore, to prevent these side effects by using MNAs to apply the desired therapeutic substances locally under the skin at the targeted dose preventing the hepatic first pass effect. Ultimately, a dissolvable polymer with the stated bioactive cargo is cast into the production molds under vacuum to produce the dissolvable MNAs. To characterize and demonstrate the performance of the fabricated needles, (i) scanning electron microscope images are taken which show the accuracy of the fabricated geometries with a 0.75%-0.80% difference from the targeted dimensions, and (ii) a series of in-vitro tests are performed including piercing, cytotoxicity, dissolution, scratch assay and HPLC. It is shown that optimized MN geometries can be precisely fabricated using the presented fabrication methodology and the fabricated MNAs have promising results regarding drug delivery and mechanical feasibility.

Özet

OSTEOARTRIT TEDAVISI IÇIN GLUKOZAMIN, KONDROITIN VE HYALURONIK ASIT IÇIN ÇÖZÜNEBILIR MIKROIĞNE DIZILERININ OPTIMIZASYONU VE ÜRETIMI

Andisheh Choupani

Mekatronik Mühendisliği, Yüksek Lisans Tezi, Temmuz 2022

Tez Danışmanı: Assist. Prof. Bekir Bediz

Anahtar Kelimeler: Osteoartrit, ilaç iletimi, mikroiğne, mikroiğne dizisi, mikro imalat, yapısal optimizasyon, sonlu elemanlar analizi.

Hipodermik enjeksiyonlar ve oral ilaçlar gibi geleneksel ilaç dağıtım sistemlerine kıyasla çeşitli avantajları nedeniyle, mikroiğne dizileri (MNA'lar) umut verici bir ilaç dağıtım sistemidir. İğne geometrisi, MNA'nın performansını etkileyen önemli bir faktördür. Bu nedenle, sayısal modeller geliştirmek ve iğne geometrisini optimize etmek oldukça önemlidir. Bu çalışmada, MNA'ların optimum tasarımını belirlemek için çok amaçlı bir optimizasyon çerçevesi sunulmaktadır. Bu amaçla, dikilitaş geometrisine sahip tek bir mikro iğnenin (MN) üç boyutlu modeli geliştirilmiştir. Deriyi delme sürecini simüle etmek için iğnenin uç bölgesine bir yük uygulanmaktadır. Kuvvetin oryantasyonuna bağlı olarak, burkulma veya bükülme nedeniyle yapıda kırılma olabileceğinden, iğne genişliği, uç (tepe) açısı, taban köşe yarıçapı gibi geometrik özellikleri elde etmek için baskın olmayan sıralama genetik algoritması II'ye (NSGA-II) dayalı çok amaçlı bir optimizasyon gerçekleştirilmiştir. Buradaki amaç, iğnelerin deriye sorunsuz bir şekilde girmesini sağlamaktır; bu nedenle amaç fonksiyonu, yapı boyunca meydana gelen maksimum gerilmeyi en aza indirecek şekilde ayarlanmıştır. Sonuç olarak, seçilen boyutlar 8.8'lik bir güvenlik faktörü sağlar. Daha sonra iğnelerin optimize edilmiş geometrisi kullanılarak, MNA'lar için ana (erkek) kalıplar mekanik mikro işleme prosesi kullanılarak PMMA'dan üretilmiştir. Bu imalat yöntemi, temel olarak geometri yeteneği, üretim hızı, üretim maliyeti ve kullanılabilecek malzemelerin çeşitliliği nedeniyle seçilmiştir. Üretilen ana kalıplar, mikro kalıplama yaklaşımıyla Polidimetilsiloksan (PDMS) üretim (dişi) kalıplarını imal etmek için tekrar tekrar kullanılabilmektedir. Bu çalışmada, MNA'ların üre-

timinde kullanılan malzemeler esas olarak Osteoartrit (OA) uygulama amacı için ele alınmıştır. Osteoartrit en yaygın artrit türü olup eklem kıkırdağının yanı sıra sinovyal eklemin bileşenleri olan subkondral kemik, sinovyum, eklem kapsülü ve başta bağlar olmak üzere eklem çevresi yumuşak dokuları da ilgilendiren dejeneratif ve destrüktif bir kronik hastalıktır. Osteoartrit tedavisinin temel amacı eklemin yapı ve işlevlerini korumak, inflamasyonu ve fibrozisi azaltmak ve progresif kıkırdak kaybını önlemektir. Glukozaminoglikan (GAG), Kondroitin (CS) ve hiyaluronik asit (HA) içeren, hasara uğramış kıkırdak matris bileşenlerinin yerine konmasını hedefleyen medikal destek tedavileri, cerrahi olarak eklem replasmanına gitmeyi önleyici rejeneratif stratejiler arasında yer almaktadır. Dolayısıyla GAG ve CS'in ağrıyı azaltabilmesi için ağız yoluyla yüksek dozda, sürekli ve haftalar-aylar boyunca alınması gerekir. Ancak bu alım gastrointestinal sistemde yan etkiye yol açabilir. Bu nedenle MNA'lar kullanılarak hedeflenen dozda deri altına istenilen tedavi edici maddeler lokal olarak uygulanarak hepatik ilk geçiş etkisi engellenerek bu yan etkilerin önlenmesi amaçlanır. Son olarak, belirtilen biyoaktif kargoya sahip çözünebilir bir polimer, çözünebilir MNA'ları üretmek için vakum altında üretim kalıplarına dökülür. Üretilen iğnelerin performansını karakterize etmek ve göstermek için, (i) taramalı elektron mikroskobu kullanılarak üretilen iğnelerin geometrileri incelenmiş ve hedeflenen boyutlardan 0.75%-0.80% farkla fabrikasyon geometrilerin doğruluğunu gösterdi, ve (ii) bu iğneler kullanılarak yapay delme, sitotoksisite, çözünme, çizik testi ve HPLC dahil olmak üzere bir dizi in vitro test gerçekleştirilir. Optimize edilmiş MN geometrilerinin sunulan üretim metodolojisi kullanılarak hassas bir şekilde üretilebileceği ve üretilen MNA'ların ilaç dağıtımı ve mekanik fizibilite konusunda umut verici sonuçlara sahip olduğu gösterilmiştir. testleri yapılmıştır.

Acknowledgements

Foremost, my deepest gratitude and appreciation goes out to my advisor, Dr. Bekir Bediz, for his dedicated support, guidance, motivation and immense knowledge throughout my masters study and research.

It is my pleasure to thank and acknowledge Prof. Feza Korkusuz, Prof. Petek Korkusuz, Dr. Feray Bakan Misirlioglu, Dr. Meltem Sezen, Dr. Busra Tugba Camic, and Prof. Guralp Ozkoc who provided us with the knowledge and insights that enabled us to carry out the project.

I would like to thank Sabanci University for providing me the privilege and opportunity of completing my masters studies.

I would also like to express my gratitude to the Scientific and Technological Research Council of Turkey (TUBITAK), for supporting our project under Grant No. 120R022 (PI: Bekir Bediz).

I wish to extend my sincere thanks to Elif Sevval Temucin for her support, and assisting me through every aspect of this project.

Many thanks to Eda Çiftci Dede for her efforts and contribution in performing the MTT and scratch assays for our project.

I also wish to thank Iskefe Holding for their support in the fabrication of artificial skin samples, Nobel Pharmaceutical Company for carrying out the HPLC test, Ertugrul Sadik and Suleyman Celik for their assistance in the fabrication of master molds.

And finally, my friends: Mahsa, Meisam, Peiman, Kazi, Naeimeh, Arash, Suzan, and Negin for their enthusiasm and friendship.

Dedicated to my family
for their support and encouragement.

Table of Contents

List of Tables

List of Figures

Chapter 1

Introduction

Chapter 1 provides a broad overlook on drug delivery systems, their routes of administration and the sets of challenges they face. A state of the art drug delivery system known as microneedle arrays has been introduced along with their various types, materials, and geometries. A review of optimization and fabrication methods of the microneedle arrays has been mentioned as well as the many applications in which they have been used for specific treatments.

1.1 A Brief History of Drug Delivery Systems

Historically, modern drug delivery systems have been developed after ancient models, and they seem to be developing at a very rapid pace over the centuries. The origin of drug delivery approaches cannot be determined because pharmacists were practicing before the word Pharmacy was even conceived. In the early 19^{th} century, drug delivery technologies evolved from the Industrial Revolution to the present day. Various forms of medicines, including capsules and microparticles, were commonly produced on a large scale after the invention of machines [5].

In general the evolution of drug delivery systems has been divided into three distinct time periods (generations). The first generation began with the invention of sustained-release capsules. In the early 1950s, modern drug delivery technologies became more commonly available. These capsules could deliver a drug for up to 12 hours after administering the medicine orally by delivering a first dosage immediately followed by a gradual release of the remaining dose. The second generation of drug delivery systems was developed between 1980 and 2010. Even though the fact that the drug delivery systems were fascinating and had a lot of impact on the industry, they did not have a very impressive success rate according to their clinical

formulations. At the beginning of the 1980s, transdermal and oral formulations of small molecules that provided therapeutic durations of up to 24 hours were the most prevailing form of drug delivery on the market. Since 1989, long-acting injections and implants have been available, expanding the period of time for which drugs can be delivered, from days to months and in some cases even to years. The 2000s were considered to be the beginning of the nanomedicine era. There remains much work to be done on establishing the third generation of drug delivery systems, as they will need to go far beyond the second generation technologies if both physical and biological barriers are to be overcome successfully.

Despite the remarkable breakthroughs over the last several decades in drug delivery systems, there are still many technologies that have not yet been discovered nor utilized in an authorized form. With the increase in life span as well as the prevalence of various diseases, the number of people requiring long-acting treatment is increasing. It is important to innovate in this field and its technologies to address the present and future unmet needs, such as enhancing the water solubility of drugs, creating longer-lasting medications, and surpassing biological barriers. Future drug delivery technologies must draw upon past experiences to develop effective treatments [6, 7].

1.2 Drug Delivery Systems

There has been a great deal of success with converting promising therapeutics into effective treatments through delivery systems. Due to the rapid evolution of the therapeutic field, the delivery strategies and technologies were adjusted quite fast to meet the evolving needs of drug delivery [8–10]. The term "drug delivery system" refers to a wide range of technologies, compositions, manufacturing strategies, methods of storing, and approaches meant to transport a medical substance to its targeted site to obtain the intended therapeutical effects [11]. In a nutshell, a drug delivery system is the interaction between a drug and a patient. This may be in the form of a compound or substance to be administered therapeutically, or it may consist of a device that is used to deliver the drug. An important distinction must be made between drugs and devices, as this is the basis for regulated control by drug and medicine control authorities. As long as the device is administered into the body to achieve therapeutic effects through a physical process or it contains a drug to avoid complications, it's considered solely as a device. It is important to realize that there is a broad range between drugs and devices, and this determination is made on a case-by-case basis [12].

Various principles are considered when optimizing drug effectiveness, safety, and improving patient convenience and satisfaction. These include delivery route, the site of administration, metabolic rate, and toxic effects [13]. The purpose of drug delivery is to modify the bioavailability and characteristics of a drug utilizing different components, carriers, and medical devices in its formulation [14, 15].

1.3 Routes of Administration

The concept of drug delivery is often considered that it's strongly associated with dosage form and administration route, which is often viewed as being part of the definition as well. TThe concepts of drug delivery and route of administration are fundamentally different. Drug administration route corresponds to the actual pathway that a substance follows to pass into the body, while drug delivery refers to methods and devices that are used to transport a substance through the exact administration route.

An important aspect of achieving the therapeutic goal is choosing the appropriate administration route. It is therefore important to consider several factors before administering a drug, including its own characteristics, the disease to be treated, and the desired therapeutic duration [12]. Application locations usually determine the routes of administration. The most common administration routes are through the Gastrointestinal system (oral and rectal), parenteral (injected), sublingual, transnasal, pulmonary, and transdermal, yet there are a variety of ways to deliver drugs through a particular route [16]. In the following sections, a selection of the administration routes are discussed and reviewed.

1.3.1 Oral drug delivery

In terms of formulation and methodology, oral drug delivery is typically targeted on the areas within the gastrointestinal tract (GIT) [17]. Among the various route of administration, the oral route is the most preferred method for its easily digestion, painlessness, versatility, noninvasive, cost-effective, and its compliance with patient needs [18, 19]. Similarly to many other methods of drug delivery, oral administration poses its own set of challenges. Mainly two types of obstacles to oral administration are considered as: biological barriers and technological challenges. There are various types of biological barriers including, mucus, lumen, and tissue that can result in

the denaturing or non-absorption of drugs administered orally. The technical challenges are usually referred to as any obstacles that may be encountered during the production process of the oral delivery device.

In comparison with other administration routes, oral medications are more complicated in terms of absorption. In order for the oral drugs to be absorbed in the stomach, small intestine, or colon, they must be soluble in gastric fluid. Considering the slow absorption of oral drugs and the multiple barriers they must overcome, oral medication is not suitable for emergency situations [20, 21]. In addition, some drugs can be degraded before they get to the target region of absorption inside the bloodstream due to the high level of acidity and presence of digestive enzymes in the GIT. Moreover, low pH level in the digestive tract can cause many drugs to become insoluble. During the process of entering the bloodstream, the drug may be inactivated in the liver, where this could also be considered as a drawback. Other disadvantages could be referred to the release of the drugs not being controlled well (delivery sites are non-specific and side effects are not managed), macro-molecular absorption is low, and some drugs might irritate the mucous lining of the GIT causing side-effects. Up to this day still, researchers are exploring methods to include diverse technologies into oral medication compositions for better efficiency [12, 17, 22].

1.3.2 Parenteral drug delivery

Among the various ways in which the pharmaceutical substances can be administered to patients, parenteral administration is considered to be the most effective. In medical terminology, parenteral is composed of the words "para" and "enteron". By definition, this refers to the administration of drugs into the body by routes other than the GIT, but in practice, it refers to injecting substances subcutaneously, intramuscularly, and intravenously [23]. Also, many important and essential medications that are available on the medical market, can only be administered to the patient through this route, whereas other routes will not be as effective.

There are a number of advantages to parenteral administration, such as, the delivery action is initiated rapidly, it's highly predictable and mostly bioavailable, the prevention of GIT problems associated with oral drug administration, and it offers a reliable route for administrating drugs for patients with severe illnesses, who cannot ingest anything orally [8, 12, 17].

While parenteral medications offer many advantages, they are generally more ex-

pensive and complex than conventional formulations. During the preparation and administration of parenteral formulations, it is necessary to have specialized equipment, devices, and techniques [24]. Parenteral administration has many additional disadvantages such as [12, 25]:

- The pain involved with injection makes it unsuitable for delivery, where patient compliance is also an issue.
- A protein product that requires sustained levels of delivery will be troublesome when delivered by injection.
- The subcutaneous deposit makes it difficult to control the absorption rate.
- Tissue damage can occur when changing the injection site regularly to prevent unabsorbed drug accumulations.
- Possible needle injury
- Generates bio-hazard medical waste
- Specialized staff is required for injections

As a result of improvements in formulation technologies, parenteral drug delivery has made significant progress in the area of providing a predictable and targeted release of the drug.

1.3.3 Transdermal drug delivery

As opposed to oral, parenteral, and other routes of administeration, transdermal drug delivery (TDD) involves the administration of drugs through the skin for therapeutic purposes. Throughout history, placing compounds on the skin was very common for therapeutic treatments. In the present day, a variety of topical substances have been produced for the treatment of regional therapeutic disorders. In 1979, a three-day patch for the delivery of scopolamine to treat motion sickness was the first FDA-approved transdermal system for systemic delivery [26]. A few years later, TDD became more popular among the public, after nicotine patches were introduced as the earliest topical blockbuster. In the present day, transdermal patches are estimated to be manufactured in over a billion patches in a year [26].

Due to several advantages over other routes of drug administration, transdermal drug delivery has gained significant interest among researchers over the last few

decades. The use of first generation transdermal delivery systems such as ointments, creams, gels, and passive patches for the delivery of microparticle, lipid-soluble, low-dose substances has evolved to increase progressively. Clinical products have also been developed using delivery systems from the second generation, including non-cavitational ultrasound, chemical enhancers, and iontophoresis. By utilizing microneedles, thermal ablation, microdermabrasion, electroporation, and cavitational ultrasound, the third generation delivery systems target the stratum corneum of the skin as a barrier for their efficacy. It is therefor necessary that the physiological, biophysical, and morphological properties of the skin should be considered to deliver therapeutic agents through the skin for systemic effects[27].

The advantages of TDD over other administration routes are as follows [28]:

- Prevents the GIT where the medication might get absorbed.
- It prevents bioactive drug molecules from being transformed into inactivated or side-effect-causing drugs, known as the first pass effect.
- Ensures a constant plasma level
- Non-invasive and it is simple to use
- After removal of the patch from the skin, drug input can be stopped at any time.
- Non-expensive and improves patient compliance
- Enhances bio-availability
- The most suitable route for pediatric users.
- Appropriate route for unconscious and nauseous patients.
- There is a lower risk of overdose and the drug can be detected more easily.

The biggest problem encountered in transdermal drug applications is the limitation in the passage of the active substance (active molecules) through the epidermis barrier. Unless physical or chemical penetration is increased, the stratum corneum (SC) does not allow the passage of molecules larger than 500 Da [29]. To overcome this, strategies such as sonophoresis [30], fractional photothermolysis [31], thermophoresis [32], iontophoresis [33], magnetophoresis [34], electroporation [35] have been presented [26]. However, these methods have not been able to become widespread due to the costs and application difficulties encountered in clinical settings. This situation brings significant limitations to transdermal treatments and prevents the

topical application of many bioactive agents. In addition, skin irritation side effects are a very common problem in topical applications of this type [26].

To gain a deeper insight and better overview of the skin barriers function, the following section provides a brief overview of its anatomy and structure.

The skin barrier: A large portion of the human body is covered by skin [36]. Physicochemical limitations imposed by the skin limit the type of substances that are able to pass under. Furthermore, its multifunctional capabilities, the skin acts as a protective layer to prevent both the entry of external compounds and the egress of natural substances i.e. bodily fluids. The skin's multilayered structure is responsible for this barrier function (Fig. 1.1) [37].

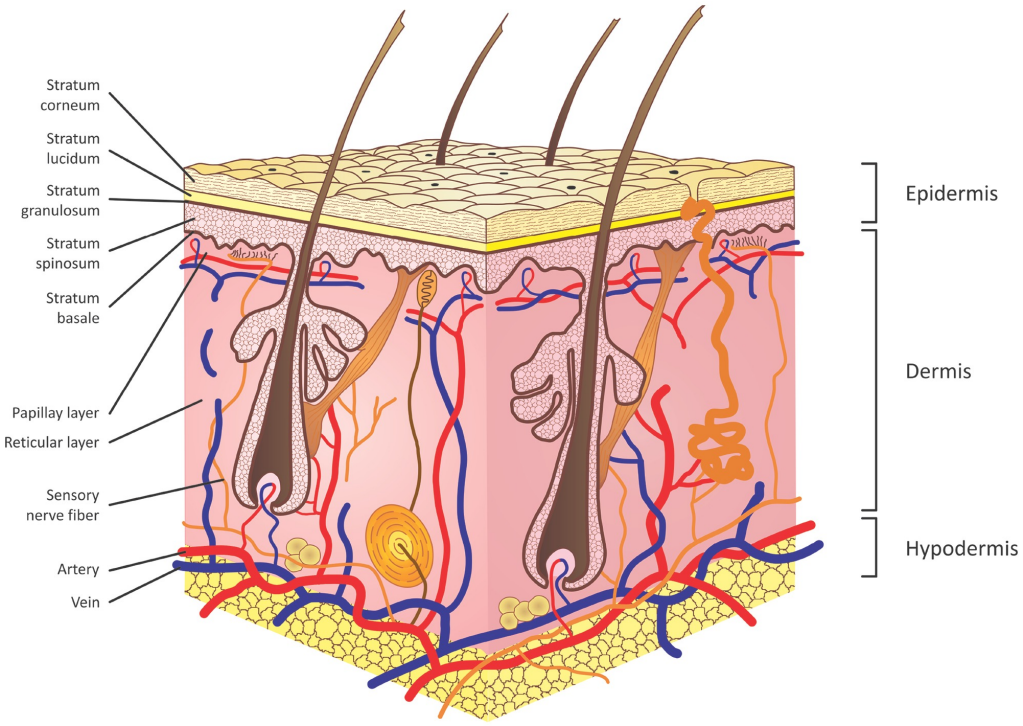

Figure 1.1: Multilayered human skin schematic [1]

The skin consists of multiple layers [38]:

- **Stratum corneum:** The uppermost layer where its thickness varies around 10-20 μm. Several levels of flattened corneocytes (dead cells consisting of a strong protein-lipid membrane) make up the stratum corneum of the human body, providing it the barrier properties.
- **Dermis:** This consists primarily of connective tissues, which regulate oxygen, body temperature, nutrients for the skin, and remove toxic substances from

the body. The thickness varies between is 2–5 mm.

- **Hypodermis:** In transdermal drug delivery, the hypodermis plays an important role. As well as holding fat tissues, it also serves as a supporting membrane for the epidermis and dermis of the skin. In order for the drug to be delivered to the systemic circulation, it must absorb through all three layers.

A state of the art technology called, microneedle (MN) drug delivery was developed in order to address the stated TDD limits and drawbacks. As a result of various research studies, it has been demonstrated that the technology is effective at delivering not just larger molecules, but also micro-molecules, cosmetics, and nano-particles [2]. In a painless and minimally invasive manner, the efficiency of drug delivery by the transdermal route could improve considerably, along with providing a broader variety of substances that are to be delivered [39].

1.4 Microneedle Arrays (MNAs)

Recent studies have suggested that micro-scale needles could be utilized to increase the skins permeability. During the application of these minimally-invasive patches, the outer skin barrier is temporarily disrupted, thereby forming small pores that penetrate the stratum corneum and the upper region of the dermis. Although microneedles was initially introduced in the 1970s, it was not only until a decade ago that the required technology for the production of micro-needles became widely accessible. By combining the advantages of parenteral injections and transdermal patches, MNAs provide a minimally-invasive route of drug delivery to the skin [40].

The height of microneedles is generally a couple of hundreds of micrometers, their width ranges from 50-400 μm and tip radius of 1-50 μm. Because of their small size, the needles do not contact the sensory nerve endings. Figure 1.2 illustrates how microneedles differ from conventional approaches such as hypodermic needles. It can also be seen that the microneedles do not reach the nerve fibers which cause the feeling of pain. Thus, they reduce the stimulation of nerves and therefore prevent the feeling of pain from being triggered unlike parenteral injections [41, 42]. Additionally, a variety of advantages of microneedles over hypodermic injections are reported in existing literature, including: a minimum risk of skin injury (e.g. microneedles do not introduce pathogens to the body nor provide bleeding), ease of application, and the ability for self administration to name a few [40, 43].

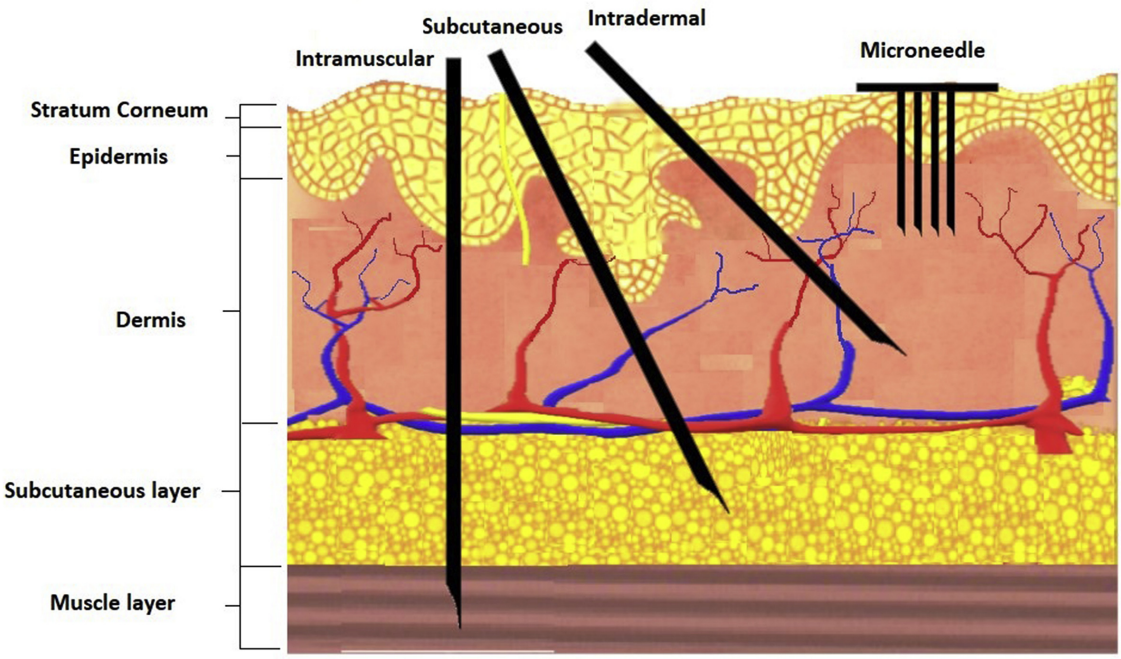

Figure 1.2: An illustration of an MNA patch piercing the skin in comparison to a conventional hypodermic needle. The MNAs penetrate the stratum corneum, allowing drugs to enter the epidermis and dermis layers without damaging nerve fibers or blood vessels [2]

Microneedles can be classified into four main groups based on their different principles and methods of penetration [44]:

- **Poke and patch:** Before applying the transdermal patch, solid nonbiodegradable microneedles are used to create microchannels.
- **Coat and poke:** Microneedles are coated with drug molecules and then inserted into the skin for drug release.
- **Poke and flow:** Pressure-driven convection is used to deliver liquid substances to capillaries in the skin through hollow microneedles.
- **Poke and release:** Microneedle structure made from biodegradable polymers with bioactive cargo, which dissolves or degrades when inserted.

1.4.1 Types, materials and geometries of MNAs

Various MNA have been designed and engineered with different geometries and materials for obtaining an effective transdermal drug delivery (see Fig. 1.3). Apart

from the common geometries such as the pyramidal and conical shape, several other geometries have been manufactured such as the circle, square, and negative bevel obelisk, under-cut, bio-inspired (e.g. snake fanged and honey-bee stinger) and many more [45–49]. Different factors such as mechanical feasibility, fabrication and skin insertion capabilities, drug dosage capacity, initiating pain, effectiveness and methods of delivery, have major impacts on the MNA designs.

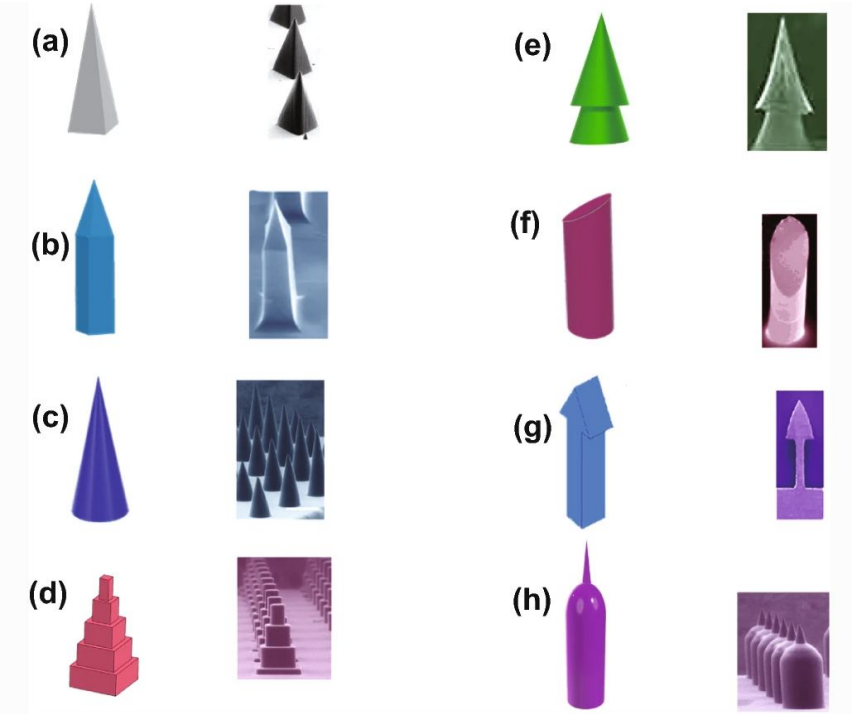

Figure 1.3: Design and shapes of different microneedles such as (a) pyramidal, (b) square obelisk, (c) conical, (d) stair-stepping, (e) arrow-head, (f) beveled cylinder, (g) under-cut obelisk, (h) turret. [3]

There are four main types of microneedles as seen in Fig. 1.4.

- **Solid MNAs:** Solid microneedles without biocargo are one of the first types and are considered as a pre-treatment of the skin, since they create micron-scaled cavities by inserting and removing them. This process involves a 'poke and patch' method, in which microchannels are formed. As a result of these microchannels, topical drugs or transdermal patches containing biocargos can diffuse directly into dermal tissue, enhancing their permeability [44, 50, 51]. Due to the early availability of micro-fabrication processes, solid MNAs were initially made of silicon, however, they have also been created from ceramics, various metals and polymers. However, recent advancements in biomaterials science and engineering as well as certain concerns regarding the effectiveness

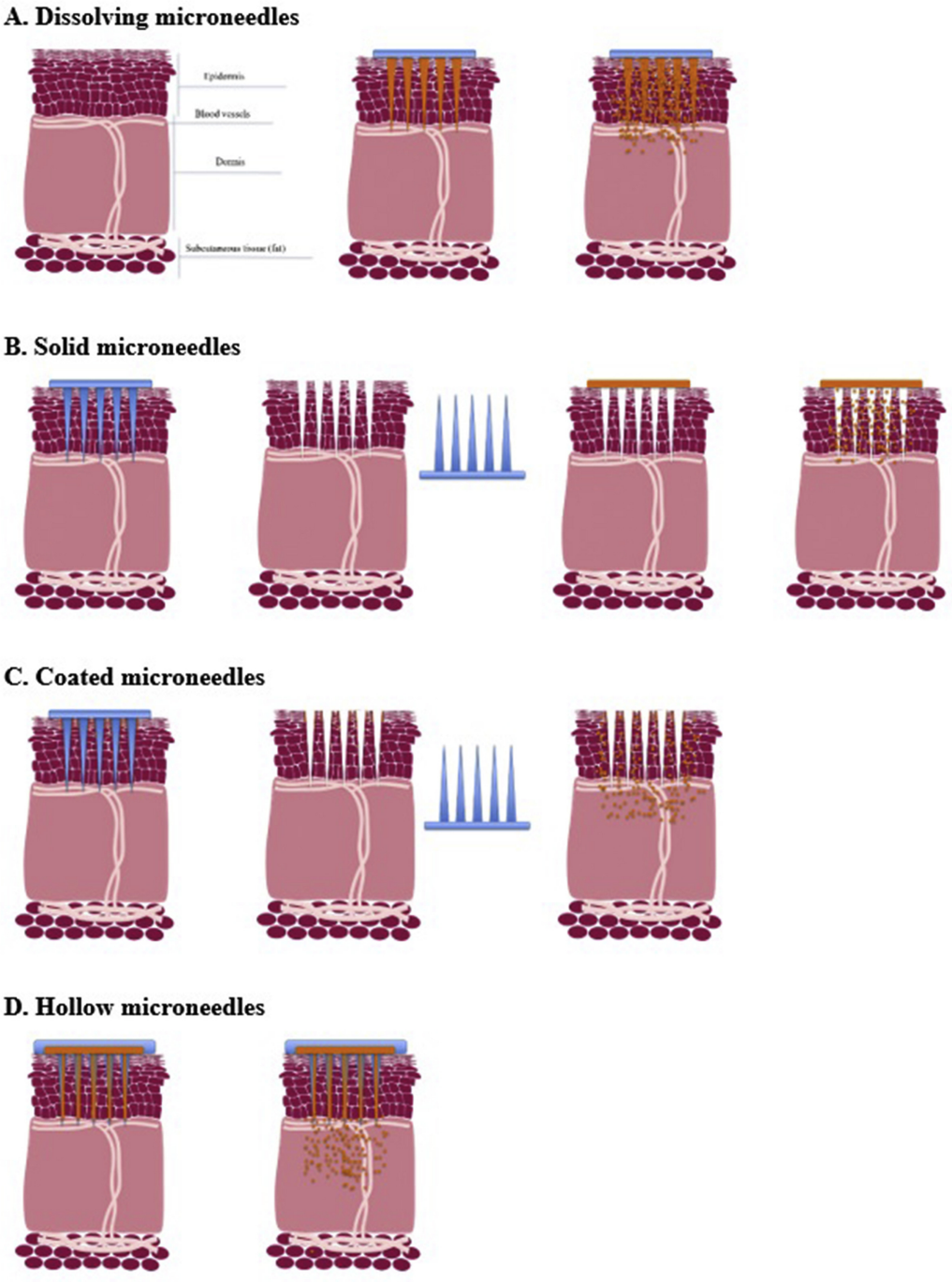

Figure 1.4: Different MNA types for intradermal drug delivery [2]

of drug delivery, application complexities, and the requirement to prepare topical drug formulations with different compounds, have been a motivation for developing other types of MNAs [44, 51–53].

- **Coated MNAs:** Microneedles that work on the coat and poke principle are coated microneedles. These biocargo coated microneedles are fabricated by a solid microneedle, as stated above, along with a coat of drug formulations.

Numerous coating methods have been presented in literature. In addition to solid MNAs, coated MNAs have also been manufactured using the same materials. By using coating formulations containing, solvents, thickening, and stabilizing agents enable an efficient and reproducible micro array coating, fast skin absorption, and durable products. Carboxymethylcellulose (CMC), polyethylene glycol (PEG), poloxamer Lutrol F68, and trehalose have been used for coating formulations [50, 54].

Coated MNAs face certain challenges, such as limitations for accurate drug dosage, decreased skin permeability due to the drug coating which cause the reduction of tip sharpness, complex drug formulations, and may cause transmitting diseases through generated bio-hazardous waste when disposal. Moreover the risk of non-dissolving microneedles breaking inside the skin during insertion, continues to be the main concern. The stated challenges have motivated researchers to develop new types of MNAs with much more advantages [53].

- **Hollow MNAs:** Hollow MNAs use the 'poke and flow' method. They are basically a miniaturized model of a hypodermic needle. Through microchannels created by microarrays across the skin layer, drugs are delivered with pressure-driven flows of liquid formulations. Due to their structure and fragility, hollow MNAs are complicated to manufacture [50, 51, 55]. Compared to other types of MNAs, hollow MNAs enable constant drug delivery and can release high dosages of biocargo. In addition, delivering liquid drug solutions is one of their advantages without requiring any dry biocargo compositions. With the reduction in the drug volume, the solution still has to be strictly considered to gain efficient drug delivery to the skin. Various materials are used in the fabrication of the hollow MNAs with a variety of features including silicon, different polymers and metals, and even glass [55, 56].

  Hollow MNAs face a series of limitations such as complex manufacturing procedures due to their complicated designs, high cost of fabrication, possible leakage of drugs, needle breakage due to fragile structure and the potential of cloggage of the microchannels within the needles. With the mentioned challenges, special considerations must be taken into account when designing and fabricating these types of MNAs [53].

- **Dissolving MNAs:** Poke and release is the principle behind dissolving microneedles. In recent years, they have gained immense attention due to their ease of manufacture and use in comparison to other types of MNAs [2, 57].

A biocompatible polymer is used for their fabrication. After application to the skin, these MNAs containing biocargo release the drug compounds into the skin's microenvironment via a rapid dissolution or a slow degradation of the polymers. Various polymers including polylacticcoglycolic acid (PLGA), polyvinylpyrrolidone (PVP), polyvinyl alcohol (PVA), PGA, PLA, CMC, sodium dextran, maltose, chitosan, and silk have been used for fabricating dissolving MNAs [51, 58, 59]. In addition to drug release, these polymers affect the fabrication process, mechanical strength and insertion stability, bioavailability, skin absorption, and durability of the MNAs.

In contrast to the other types of MNAs, dissolving MNAs do not generate biohazardous wastes due to their ability to degrade in the skin environment, thus the risk of transmitting diseases can be prevented. Many other advantages can be pointed out to their non-expensive and simplicity in manufacturing, ease of application and storing, patient compliance, and drug delivery can be controlled well. These benefits enables a suitable option for skin-targeted drug delivery [50, 51, 53].

In addition to the many benefits of the MNAs, several factors should be taken into account for enhancing the performance of the MNAs. Therefore, to achieve the desired performance, theoretical modeling, simulations, and optimization techniques must be developed. These will be beneficial for the reduction of both expenses and time costs of the fabrication process. The following section provides a better perspective on simulation and optimization strategies.

1.4.2 Optimization methods

Simulations for modelling MNAs is a field of expanding research and investigation. Although it can be realized that many of the researches have been focusing on the area of manufacturing methods and experimental aspects, the simulations and modeling approaches have been mostly neglected. Simulations could help predict the performance of the MN feasibility to guide the research efforts toward critical aspects of their development [60]. A series of MNAs have been numerically modelled for enhanced drug delivery, based on variations in morphology, materials, and designs [61, 62]. The initial numerical simulations of MNAs report back to 1999 when researchers modelled the extraction rate of fluids for hollow MNAs [63].

Among the primary objectives of MN simulations is to specify the design variables

necessary to achieve optimal MN performance. The depth of penetration and rate of drug release are the general outcomes of such modelling approaches. Both skin and MN parameters are related to these outputs [64]. Factors such as material compositions and geometrical parameters including the shape of the needle, height, width, tip radius, and density have major effects on the MNAs performance [65]. Moreover, studies show that these factors are also effective for modelling the permeability enhancement of the skin [66–68].

For penetration simulations, the MN and the skins' characteristics such as Posions ratio, Yield stress, Young's modulus and other mechanical properties must be taken into account for the model setup [69]. Typically, commercial finite element software including COMSOL, ANSYS, Preview and Abaqus are used for modeling [70–72]. A series of investigations have been conducted to characterize the behavior of MNs, including developing FEM simulations to analyze the required penetration force [73], demonstrating the generated maximum stress occurring at the tip of the MN [74], the effects of the MN dimensions and mechanical properties of the skin to model the failure and deformation of the MN [75], analysis of different sets of forces during MN (conical shaped MN) penetrating the skin [73], and predicting human skin behaviour [70].

Compared to solid MNs, the dissolving MNs composed of polymers are quite flexible. Therefore, it is essential to consider the mechanical properties of dissolving MNAs to optimize its structure for the force/pressure it can endure.

1.4.3 Fabrication methods

Microneedle arrays with optimal MN designs need to be constructed in a simple, non-expensive, and reproducible manner in order to become widely used [76]. A variety of techniques have been described in literature for fabricating and manufacturing MNAs. In general these methods are classified into two main groups including direct fabrication and mold based techniques.

Several methods of 3D printing technologies have been utilized for fabricating the MNAs directly or to produce the MNAs by micro-molding [77]. Stereolithography (SLA) is a popular method of 3D-printing which has been utilized for the cost-effective fabrication of MNAs without the need for clean room facilities. Studies show that this technique has been used for the production of master molds, and also the fabrication of solid or hollow MNAs with biocargos for drug delivery [78].

An additional method to 3D printing fabrication of MNAs, is the fused deposition modeling (FDM) method. This technique is used for directly fabricating MNAs composed of PLA along with the etching technique to enhance resolution [79]. Furthermore, 3D printing methods based on photopolymerization have been developed including digital light processing (DLP) and continuous liquid interface production (CLIP) techniques, with the capability to manufacture complicated structures with better quality in comparison to SLA and FDM. A layer by layer approach is employed for DLP method, and studies show it is used to fabricate complex MNAs and to increase mechanical feasibility. CLIP on the other hand, manufactures a part continuously, which has been stated to rapidly manufacture different geometries, dimensions, and inter-spacing of MNAs with various materials [80].

Alternative fabrication methods of MNAs can be referred to as, hot embossing, reactive ion-etching, wet chemical etching, injection molding, two-photon polymerization, and drawing lithography [81]. For the case of micro-molding method, initially a master mold is manufactured using micro-milling. Then after replica or production molds are fabricated when a polymer solution (e.g. polydimethylsiloxane-PDMS), is poured on to the master mold and cured by heating, cooling or UV light. Ultimately, biodegradable polymers are poured into the replicas and MNAs are fabricated.

1.4.4 Applications

There has been considerable progress made in the field of treating diseases, administering immunobiological therapies, diagnosing diseases, and using microneedles for cosmetic purposes [82]. It is possible to diagnose diseases with MNAs, for instance hollow microneedles are able to pierce the skin and extract the tissue fluids with vacuuming or capillary force. Studies have been done for diagnosing diseases such as cancer, diabetes, cardio-vascular diseases, thrombosis and atherosclerosis [83]. For cosmetic purposes MNAs are either used to increase skin permeability by generating microchannels, or they are used to accelerate the natural recovery of damaged skin tissue [84]. It has been demonstrated that MNAs are a reliable tool for administering immunobiological therapies such as vaccines, where they are superior to conventional methods of vaccination. Malaria, HIV, Diphtheria, influenza virus vaccines are studied with microneedles [50]. A number of research has also been done on the treatment of specific diseases with the use of MNAs, including cancer therapy, diabetes, obesity, Alzheimer's disease, neuropathic pain, and neonatal infections [82]. The following section defines an articular cartilage disorder, where

MNAs can be used for treatment.

Treatment of Osteoarthritis

Articular cartilage is a connective tissue in the joints that is non-vascularized and has a low cellular density. Injury, natural wear or tear of this issue are common causes of health problems [85]. Among these, Osteoarthritis (OA) is one of the most rampant articular cartilage disorder, impacting many individuals globally as the major cause of disability [86]. The cartilage tissue cannot be completely healed and repaired, due to its avascular nature that does not include mononuclear cells. There are many treatment methods for OA including:

- **Non-surgical:** Mechanics of the joint, changing the axis, Management of the body mass index, skeletal muscle strength, increasing exercises, Corticosteroid, and analgesic and anti-inflammatory.
- **Course shifting of the disease:** Use of glucosaminoglycan (GAG) and chondroitin sulfate (CS) supplementation, and intra-articular administration of hyaluronic acid (HA).
- **Cellular:** Platelet-rich plasma, platelet-rich growth factor, stromal vascular fraction, stem cells, and extracellular vesicles.
- **Surgical:** Mosaicplasty, Allograft, Autologouse chondrocyte implantation, high tibial osteotomy, partial or total joint replacement surgery.

The goal of OA therapy is to keep the joint's structure and functioning maintained, minimize inflammation and fibrosis, and avoid cartilage loss. The commonly used Anti-inflammatory medications, temporarily reduces OA symptoms while causing several side effects [87]. Medical support treatments have aimed for replacing damaged cartilage matrix components with bioactive materials such as GAG, CS, and HA [88]. These biocomponents are mostly injected into the joint with a hypodermic needle, resulting in changes in muscle strength, balance and gait pattern as well as reducing pain. Moreover, such injections may cause abrasion on the skin, and have undesirable side effects occurring with continuous use. Another disadvantage is the need for the injection to be performed in the presence of an expert in an invasive procedure that requires sterile hospital conditions.

The stated limitations reveal the need to administer GAG, CS, and HA alone or in combination, at much lower doses, with an approach that will provide a long-acting and keeping the plasma level constant. The use of intradermal MNAs may be advantageous in reducing or instantly eliminating possible side effects and toxicity and

increasing the patients' compliance with the drug administration. It is considered that the current work addresses the development of MNAs as a treatment for OA disease for the first time.

1.5 Hypothesis and Objectives

Our hypothesis in this study is that microneedle arrays are capable of delivering GAG, CS, and HA locally into the skin for the treatment of OA. Therefore, to prove this statement, a set of goals have been set:

- Geometry of the needles needs to be optimized to achieve painless insertion and reduce structural failures of microneedle arrays. The optimized geometry is selected to be an obelisk geometry due to its ease of manufacture.
- A simple, fast, and low-cost fabrication method based on mechanical micromachining and micro-molding needs to be implemented. In this step, tip loaded MNAs are fabricated and scanning electron microscopic images are taken for the geometry characterization.
- In-vitro tests including penetration, dissolvability, drug dosage, cell viability and wound healing need to be performed to demonstrate the fabricated MNAs.

1.6 Thesis Outline

- A detailed discussion of the optimization study, as well as the step by step fabrication process for the master mold, production mold, and microneedle array patches, is presented in **Chapter** 2. This chapter also illustrates the characterization of the master molds and microneedle array patches.
- **Chapter** 3 represents all of the in-vitro tests which were carried out in demonstrating the manufactured microneedle array patches performance.
- Ultimately, conclusions are stated in **Chapter** 4 along with recommendations for future work to be carried out.

Chapter 2

Optimization and Fabrication of Dissolving Microneedle arrays

2.1 Optimization study

As mentioned in the previous chapter, MNAs are a rapidly developing technology for user-friendly and minimally invasive drug delivery and medical applications. Simple, low-cost, and reproducible fabrication of MNAs with optimal microneedle geometry designs is crucial for their widespread adoption. The following sections provide an optimization study and the MNA fabrication process.

2.1.1 Microneedle model

Since the MNAs are intended to deliver bioactive cargo into the skin, the microneedle geometry should be able to easily pierce the stratum corneum [46]. To achieve this, the tip of the microneedle must be sufficiently sharp. A blunt tip is more likely to require a greater amount of force to pierce the upper layer of the skin when compared to a sharper tip [89]. It is also necessary to adjust the microneedle length according to the target location of the biocargo substance to be delivered. Moreover, the thickness must also be taken into account, whereas a thin microneedle is prone to breaking easily and will also have a smaller volume for containing drugs in comparison to a thicker microneedle. Therefore, the design of the MNAs and its master mold is of great importance to overcome the breakage problem and to deliver the bioactive substance to the target area without any issues.

It is essential to consider the capability of the manufacturing method when designing

microneedles geometry. For example, pyramid or conical microneedle structures can be fabricated by lithography, which is one of the most common used production methods in the literature [74]. While it is considered to fabricate the master molds with micro-milling technique, as an alternative, it is stated that an obelisk geometry is more suitable in terms of manufacturing, piercing the upper layer of the skin and carrying the drug [90]. With the obelisk geometry, the stem length can be easily adjusted according to the target region and more biocargo substances can be contained. Therefore, for each bio cargo substance to be transported, the size of the MNA (total amount of microneedle on a patch and the distance between each microneedle), the thickness, length and the tip radius of the microneedle geometry, must be determined separately.

When designing the MNAs, it is possible to consider a single microneedle as the basis for modelling purposes, since the results will be a representation of all the arrays available on the patch. In the design of the square obelisk geometry of microneedles, the main geometry parameters are the height, width, and the apex angle. Additionally, a fillet has been added to the bottom edge of the stem, which is proven to enhance the structural properties of the microneedle [46]. As shown in Fig. 2.1, the total height is indicated as h_t, and divided into sections specified as h_s for the height of the stem and h_p for the height of the pyramidal tip. The angle of the apex is defined as α, r denotes the radius of the fillet at the base of the stem, and w indicates the width of the microneedle. In the optimization analysis, all of these geometric parameters are used either as design parameters or constraints. It is also important to note that the total height $(h_s + h_p)$ of the microneedle is considered constant as 700 μm, since the MNAs are targeted to deliver the drug to a specific region in the skin. However, stem height (h_s) and the pyramidal tip (h_p) can be adjusted accordingly to obtain an optimal geometry.

During the penetration of the microneedle to the skin, it is subjected to vertical and/or lateral forces. Theoretically, only vertical forces are expected to develop during insertion, but lateral forces are also generated due to the uneven skin surface and/or failure to properly align the microneedle patch with the skin surface. This may cause failure to occur due to bucking (by vertical forces) and bending (by lateral forces) in the microneedle structure. Thus, it may be possible for the needles to break without even piercing the skins uppermost layer. To address this, the geometry of the microneedle as well as the properties of the material should be designed appropriately. This design process of microneedle geometry is performed based on finite element (FE) analysis. For this purpose, COMSOL Multiphysics FE software is implemented. To construct the FEM, tetrahedral and hexahedral

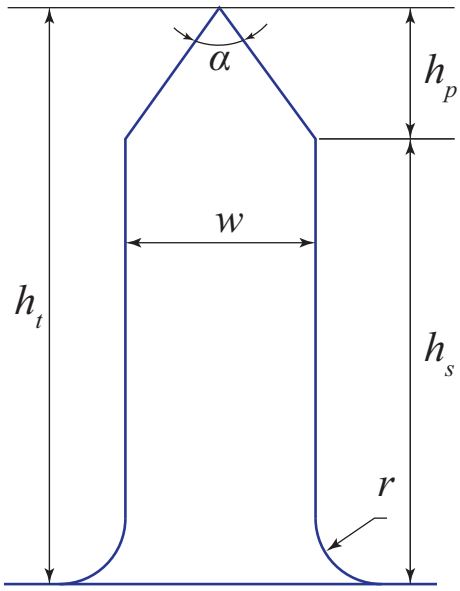

Figure 2.1: Micro-needle array and micro-needle geometry schematic.

elements are used and linear elastic material properties are applied.

The optimal outcome also depends on the material property of the needles. A bio-compatible and biodegradable polymer which is obtained from a combination of PVP and PEG 400 is used for the fabrication of MNAs. The polymers were selected based on their suitability for the chosen production method. PVP is a water-soluble, cross-linked, bio-compatible polymer that is FDA-approved for drug delivery applications [91]. On the other hand, the rigid and brittle nature of PVP makes its stiffness less suitable for microneedle material when used alone, and it has been reported in the literature that it breaks when piercing the skin [92]. To reduce the brittleness of PVP, it needs to be plasticized with low molecular weight PEG (such as PEG400, PEG1000 and PEG8000). Likewise, PEG is another water-soluble, bio-compatible and FDA-approved polymer [93]. PVP and PEG were mixed in different ratios and the polymer was prepared by adding PEG at the ratio of 0.0048 $\%w/w$. Ethyl alcohol was used as a solvent due to its easy solubility. Based on the performed mechanical tests, the mechanical properties of the polymer are given in Table 2.1. Moreover, the yield stress of the polymer is approximately 62 MPa.

For the first stage, an FE model was created based on the specified parameters and material properties to determine the microneedle geometry. Figure 2.2 shows the generated FEM. For determining a sufficient number of elements for the analysis, a convergence study was performed (see Fig. 2.3).

Table 2.1: PVP/PEG polymer material properties.

Material property	PVP/PEG Polymer
Young's Modulus, E, [GPa]	1
Density, ρ [kg/m^3]	1600
Poisson's ratio, ν	0.3

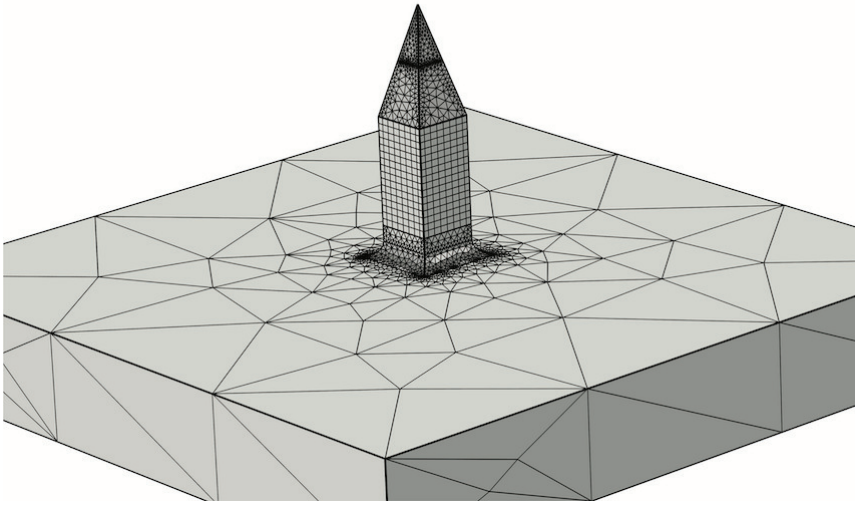

Figure 2.2: Micro-needle finite element model.

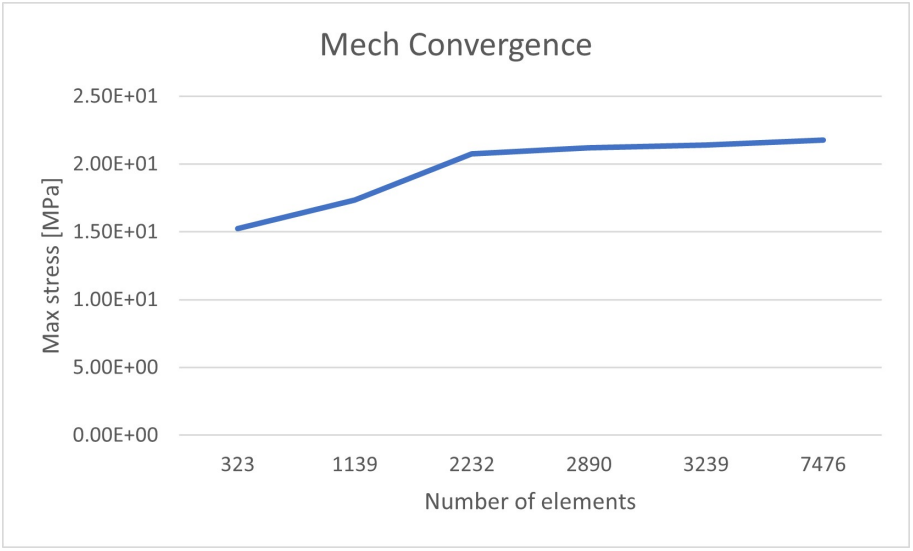

Figure 2.3: Mesh convergence results

During the development of the model, the boundary conditions were set up so that the bottom base (backing layer) of the microneedle was fixed in all directions while

only a force was inserted to the pyramidal tip region. The force during insertion was taken as 20 mN according to literature studies and applied to one third of the pyramid length [94]. To prevent the microneedle from breaking, the force was applied horizontal as the worst-case scenario. In order to find the appropriate geometry of the microneedle, an optimization study was carried out which the following section provides a detailed explanation of this concept.

2.1.2 Optimization Problem

The concept behind an optimization problem is basically the process to maximize or minimize a function with respect to a set of options, which is typically a range of possibilities obtainable in a given situation. Using the function, it is possible to compare the different alternatives to determine which option might be "the most optimal". In general, there are three basic components of an optimization problem. The first element consists of an objective function for which a maximum or minimum should be achieved. The second component is a set of design variables that could be modified to achieve an optimal objective. The third component is a collection of constraints, which are limitations on the design variables where the possibilities can range.

When designing a microneedle, the key factor of a suitable structure is considering the mechanical feasibility as well as having proper dimensions for its ease in penetration. To prevent breakage and deformation of the microneedle, the maximum stress, usually the Von-Mises stress, must be below the yield stress of the material. Secondly, for having a smooth and pain-free penetration into the skin, the width of the microneedle must be adjusted accordingly. In spite of the fact that a small structure penetrates the skin, micro-sized pores appear within the skin and their size directly correlates with the thickness of the microneedle. Therefor, the width of the MN (w) and the Von-Mises stress are selected as the design objectives, where the former is necessary to decrease the insertion area; and the latter is critical to enable failure-free insertion of the needles. Since we have two objective functions in total, a multi-objective optimization needs to be taken into account. Note that the total height of the microneedle is constant, thus the height of the stem (h_s) and pyramidal tip (h_p) can only vary within a certain range. Also, the apex angle (α) and the fillet radius (r) should be considered since the alteration of the apex angle will effect the penetration force and the width of the microneedle accordingly, while the fillet will impact the mechanical feasibility of the microneedle. These geometry parameters

are defined as the design variables, and their ranges of variation are considered as the constraints of the optimization problem which are reported in Table 2.2.

Table 2.2: Defined ranges for the geometry parameters of a MN.

Parameter	Lower bound	Upper bound
w	100 μm	350 μm
α	15°	45°
h_p	100 μm	350 μm
h_s	350 μm	600 μm
r	5 μm	50 μm

A generalized formulation of the multi-objective problem is presented as follows.

$$\begin{aligned} \text{minimize} \quad & f_1(x) = \sigma\,,\ f_2(x) = w \\ \text{find} \quad & x = \{h_p, r, \alpha\} \\ \text{subject to} \quad & 15 \leq \alpha \leq 45 \\ & 100 \leq h_p \leq 350 \\ & 5 \leq r \leq 50 \\ & 100 \leq w \leq 350 \\ & h_s \geq 350 \\ & h_s + h_p = 700 \end{aligned} \tag{2.1}$$

where σ is the Von Mises stress, $\mathbf{f}$'s, and $\mathbf{x}$ denote the objective functions and design variables, respectively.

2.1.3 Multi-objective Optimization Algorithm

Conflicts between objectives can cause difficulties in solving the multi-objective problem. That is, improving one goal can simultaneously decrease the other. In literature, numerous methods for multi-objective optimization have been presented. These methods can be grouped as *Random methods* and *Non-random methods*. Due to their highly efficient computational capability, random search methods such as genetic algorithm and particle swarm optimization have become popular among others [95]. Since, Eq. (2.1) defines a multi-objective optimization, a genetic algorithm is used to obtain the optimal dimensions for the microneedle. This algorithm uses a

version of non-dominated sorting genetic algorithm (NSGA-II) to create the Pareto optimal solutions [96]. Although multi-objective algorithms based on non-dominated sorting face various difficulties and obstacles such as complicated computations and the necessity for denoting a shared parameter, the NSGA-II, successfully deals with all the mentioned difficulties [96]. The NSGA-II is a fast and elite form of the genetic algorithm which is capable of finding a considerably improved expansion of solutions and enhanced convergence near the Pareto-optimal front.

Before, going through the algorithm steps, it is best to know the basics and definitions which are provided below [97]:

- **Domination:** When both condition 1 and 2 of the following are true about a decision variable $\mathbf{x}_1$, it is said that solution $\mathbf{x}_1$ dominates solution $\mathbf{x}_2$:

  Condition 1: For all objectives, $\mathbf{x}_1$ should not be worse than $\mathbf{x}_2$
  Condition 2: At least one objective of $\mathbf{x}_1$ is superior to $\mathbf{x}_2$

- **Pareto-optimal:** The pareto-optimal decision variable/objective function is one in which there are no other decision variable/objective function that dominate it in any way.

- **Pareto-optimal set:** Consists of a non-dominating decision variable set (Pareto-optimal) of the whole feasible search space.

- **Pareto-optimal front:** Consists of a non-dominating objective function set (Pareto-optimal) of the whole feasible search space

- **Crossover/recombination:** The crossover operator is used for creating new offspring by combining the genetics of two parents. This operator arbitrarily picks one point among two arbitrarily chosen parents and separates them and swaps them to create new individuals.

- **Mutation:** The mutation operators are used to provide diversity in simulated populations. As a method of avoiding local minima, mutation operators prevent individual populations from resembling one another.

- **Crowding distance:** A value that determines the size and density of the largest cuboid surrounding any point without taking into account any additional points in the population.

- **Crowded Comparison:** If and only if the decision variable $\mathbf{x}_1$ has the largest crowded distance, then it dominates all the members of the Pareto-optimal set.

To obtain the Pareto-optimal set as well as the Pareto-optimal front with using

NSGA-II, the algorithm goes through several steps as provided below [97]:

Step 1: First, a random parent population, P_0 , is generated and its size is assumed to be n_p.

Step 2: Then, dominance analysis is performed with each individual across the population. The number of individuals m_i, (which dominates each individual i) along with a collection of individuals, S_i (that are dominated by the individual i), are computed. All of the individuals from P_0 with $m_i = 0$ are considered as the first front, F_1.

Step 3: Then, a subtraction of one is made to the m_j value of each individual from F_1 which is linked to the $j^{[}th]$ individual and S_i. When m_j of each j individual is zero, another list denoted by H is created.

Step 4: After all members of F_1 are verified, the remaining members of list F_1 are arranged to be members of the first front.

Step 5: When the algorithm is repeated for the entire population, each individual is assigned a fitness value based on its level of non-dominance.

Step 6: Following the start of the procedure, C_0 is generated as a population of children with the size n_c using crossover and mutation operators.

Step 7: Then, after selecting individuals arbitrarily, two new individuals $(\mathbf{x}_{1,n}, \mathbf{x}_{2,n})$ are created, each considered as a linear combination of parents as given below:

$$\begin{cases} \mathbf{x}_{1,n} = \alpha \mathbf{x}_1 + (1-\alpha)\mathbf{x}_2 \\ \mathbf{x}_{2,n} = \alpha \mathbf{x}_2 + (1-\alpha)\mathbf{x}_1 \end{cases} \tag{2.2}$$

Here, α is an arbitrarily selected number between 0 and 1. For the mutation step of the algorithm, the operator uses an arbitrary real value that randomly changes the m^{th} member of the chosen vector and creates a new member [98].

Step 8: Following the creation of the first generation, for the t^{th} generation $(t > 1)$, the process changes to consist of combinations of populations $(R_t = P_t \cup C_t)$. The R_t population is organized based on the provided procedure. By adding individuals from the first front until the number of members reaches n_p, a new population P_{t+1} is formed.

Step 9: Ultimately, a crowded comparison operator is then used to arrange the individuals from the final approved front.

2.1.4 Optimized Geometry and NSGA-II Results

To obtain the optimal design variables including the height of the pyramidal tip, the apex angle, and the fillet radius according to the optimization study, the crossover and mutation probability are selected as 0.7, and 0.4, respectively. The population size is set to be 200 and 20 generations have been searched. The optimization algorithm is ran by linking MATLAB and COMSOL Multiphysics, simultaneously. In Fig. 2.4 the results of the optimizations, including the non-optimal solutions and Pareto-optimal front are shown. The objective functions are shown as the width and safety factor calculated by the ratio of yield stress of the MNAs to the maximum Von-Mises stress occur in the structure.

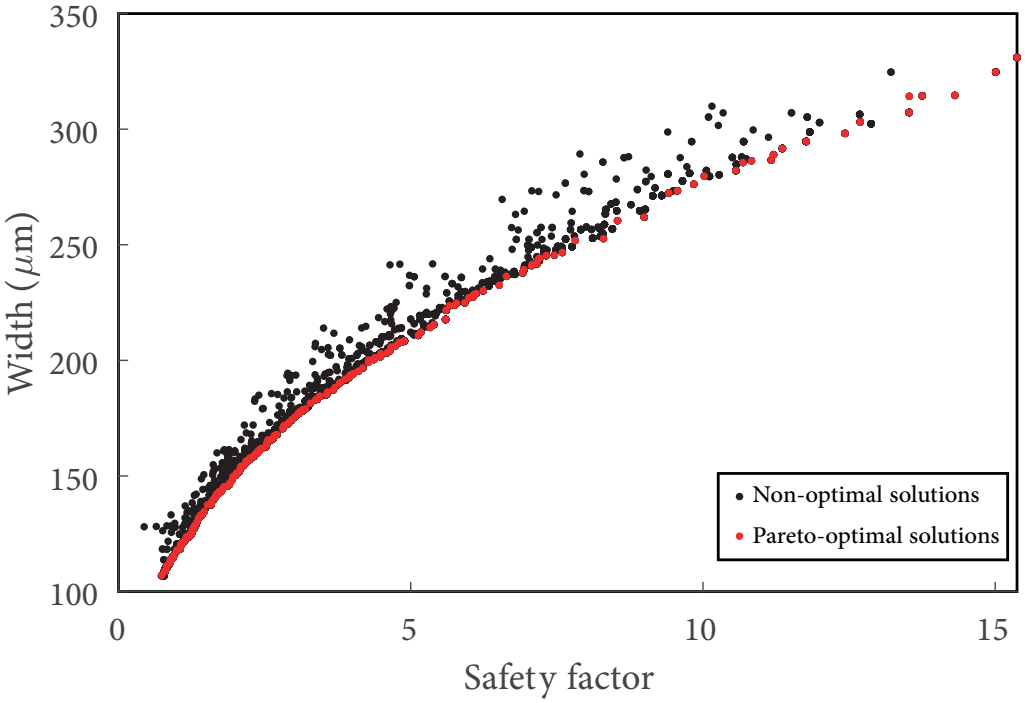

Figure 2.4: Results of the optimizations, including the non-optimal solutions and Pareto-optimal front.

Each point on the Pareto-optimal front relates to a specific set of design variables. Figure 2.5 shows three selected Pareto-optimal decision vectors on the Pareto front. Since, no weights are assigned to each objective function, the designer can select the suitable design regarding the importance of the objectives from the given Pareto optimal solutions. In accordance with the optimization study, a microneedle design that can take sufficient amount of drug and will not break during piercing the skin, with a safety factor of 8.8 and a width of 264 μm has been chosen. Table 2.3 lists

the geometric features of the selected design.

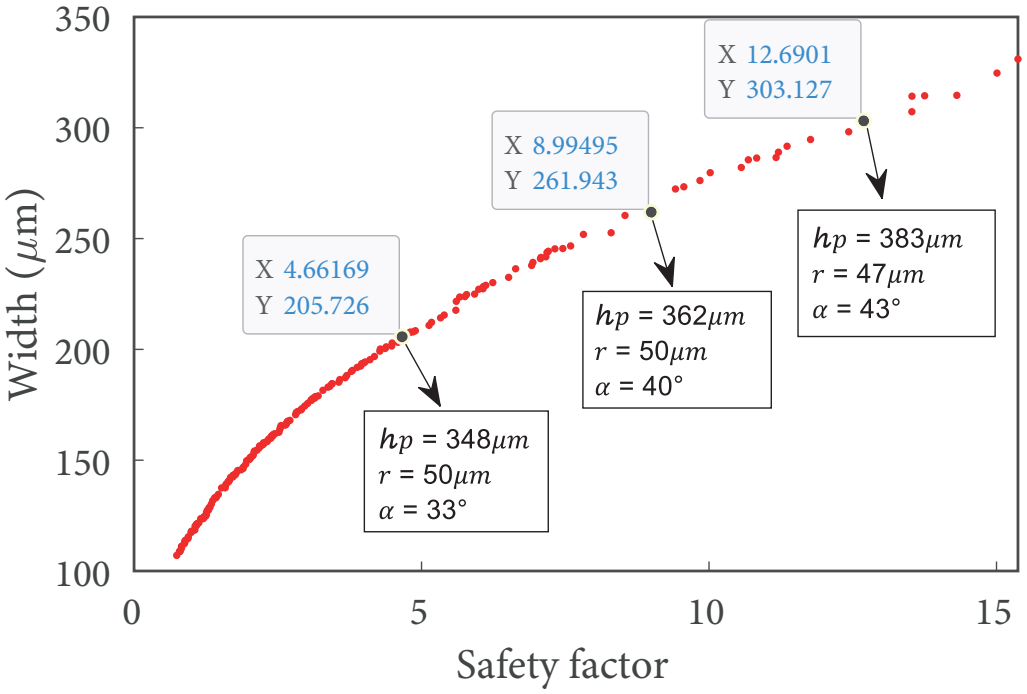

Figure 2.5: Pareto optimal solutions and corresponding three possible design parameter vectors.

Table 2.3: Selected parameters and microneedle dimensions.

Parameters	Microneedle dimensions
Total height	700 μm
Apex Angle	37 °
Width	264μm
Fillet Radius	50μm

During the optimization analysis, static analysis is performed using COMSOL Multiphysics. For example, Figure 2.6 illustrates how stress is distributed within the optimized microneedle. The values of the stress can be followed by the color bar next to the figure. Its observed that the maximum stress is occurring at the root of the microneedle stem where because of the sharp edges concentration of stress is taking place. Therefore addition of the fillets with a radius r to reduce this concentration of stress is necessary.

2.1.5 Effect of Force Angles

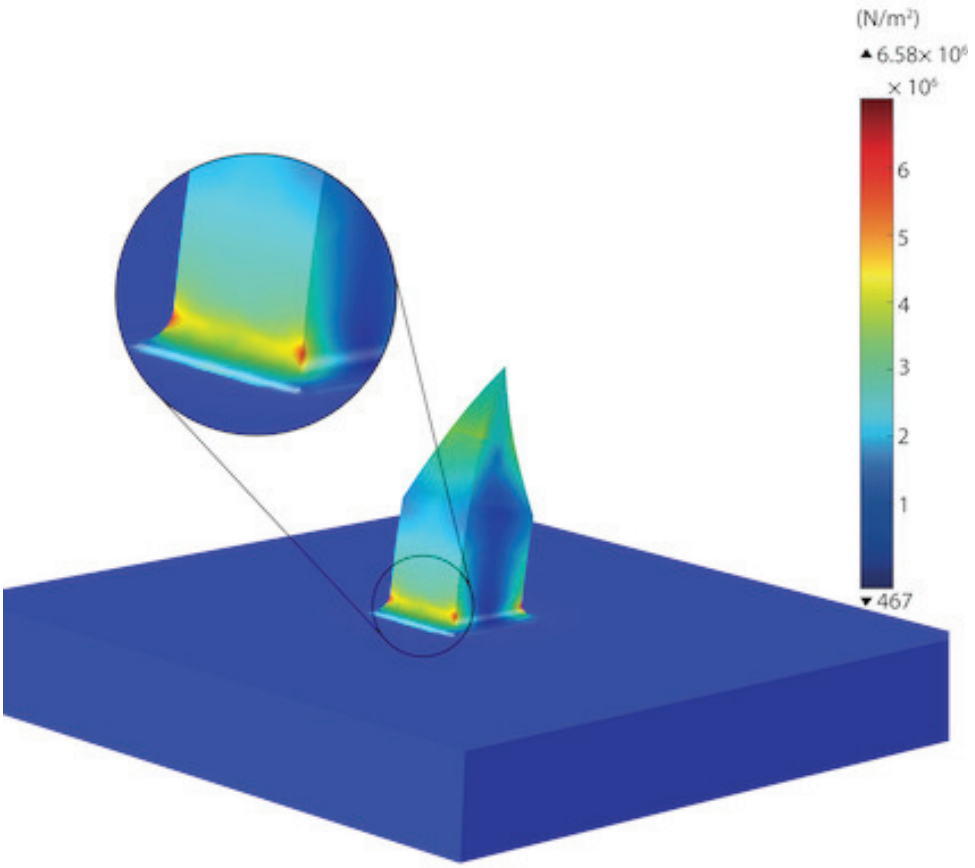

Figure 2.6: Stress distribution of the optimized microneedle geometry.

During the insertion of MNAs into the skin, buckling and bending may occur as a consequence of the force that is exerted on the microneedle from various angles. In this section, the described multi-objective optimization is solved by NSGA-II. The only difference is that the simulation is ran for comparing the buckling and bending values at different angles of forces. The algorithm calculates the values of the critical buckling factor and then compares it with the calculated bsafety factor defined as the ratio of the yield stress to the maximum bending stress (Von-mises) obtained by COMSOl. Then, the one that is critical, in other words the case that cause the microneedle to fail first is found and the objective is to maximize that value. The Pareto-optimal design for microneedles is similar to the previous one in terms of the designer's ability to choose microneedle dimensions, but this time the designer is able to make a decision based upon both the force angle and the failure criteria. Figure 2.7 shows the results of this analysis. In this figure Pareto-optimal solutions for different force angles with a constant apex angle of 30°are shown. As an example for the case of the force angle of 15°, two solutions are chosen and the corresponding values of the decision variables are shown.

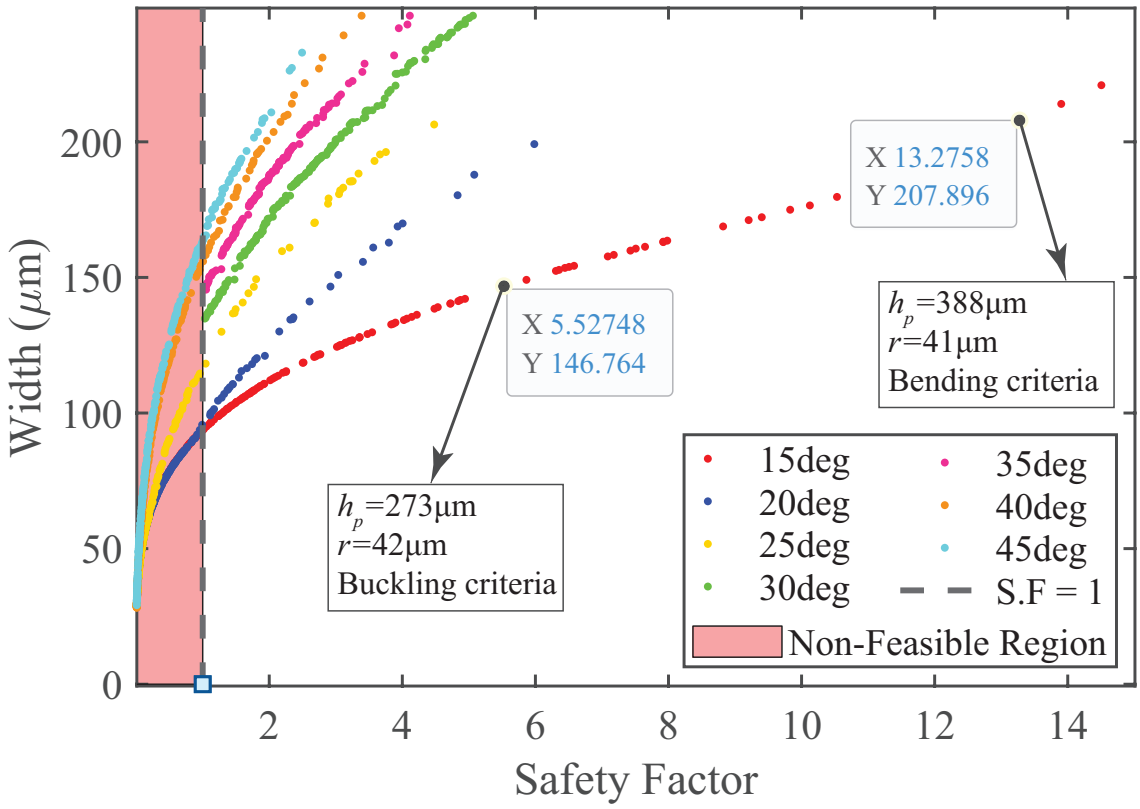

Figure 2.7: Pareto optimal solutions for different angles of force and corresponding possible design parameter vector.

2.2 Fabrication process

The fabrication process in this study employs the 'mold-based technique'. There are four main steps in fabricating MNAs with this technique. The first is to initially construct a CAD model where based on this, with the help of computer aided production software, master molds are fabricated using micro-manufacturing techniques. Afterwards, negative elastomer molds, also known as production molds, are fabricated through (micro-)molding. Ultimately, final dissolvable MNAs are fabricated from the production molds using the micro-casting technique.

2.2.1 Fabrication of Master Molds

There has been a considerable amount of research done in the literature regarding the different production methods that have been used to fabricate master molds. However, in recent years, methods with higher geometry capability, lower fabrication

time and cost have emerged. The most important of these methods are micro machining and additive manufacturing technologies.

To fabricate the MNA based on the optimized dimensions, micro-milling method was used to produce the master molds due to its production speed, production cost and the variety of materials and geometries that can be used for the fabrication. The manufacturing process on these machines is similar to that of conventional mills; however, during the machining process, cutting tools with a tip radius of 100-1000 μm are to mechanically remove chips.

The initial step of manufacturing the master molds, is to construct a CAD model. A 2×2 master mold model with the optimized dimensions and needle to needle spacing of $700\mu m$, was designed in SOLIDWORKS as shown in Figure 2.8. Thenafter, required production codes (G codes) are created by means of computer aided production software (SolidWork-CAM) to carry out the production process on micro-machine-tool (μMT). The surface roughness (R_a) of the microneedle master molds should be less than 200 nm so that the microneedle molds to be produced are of high quality and the production molds, which are the next step, should be easily separated from the master molds at the same time. Surface roughness and quality in the micro-milling process depend on the forces generated between the cutting tool and the workpiece during cutting, as shown in Fig. 2.9. These cutting forces also depend on the speed of the cutting tool to be used, the feed rate of the cutting tool on the workpiece, the depth of cut and the material being cut.

For this purpose, PMMA material is chosen for the production of master molds due to its ease of fabrication [99]. The surface roughness of the base of the needle is also measured for the produced master molds, and the R_a value is obtained as 158. Figure 2.10 shows the finalized manufactured master mold. As a result of the 2×2 design pattern of the master mold, four production molds can be fabricated simultaneously. There exists a 20×20 array of microneedles on a master mold, so that a noticeable amount of drug can be added to each patch considering the total volume of needles.

After the fabrication process, the master molds are cleaned using ultrasonic cleaning bath for 45 minutes in 35°C, to remove any chip residues.

2.3 Characterization of Master Molds

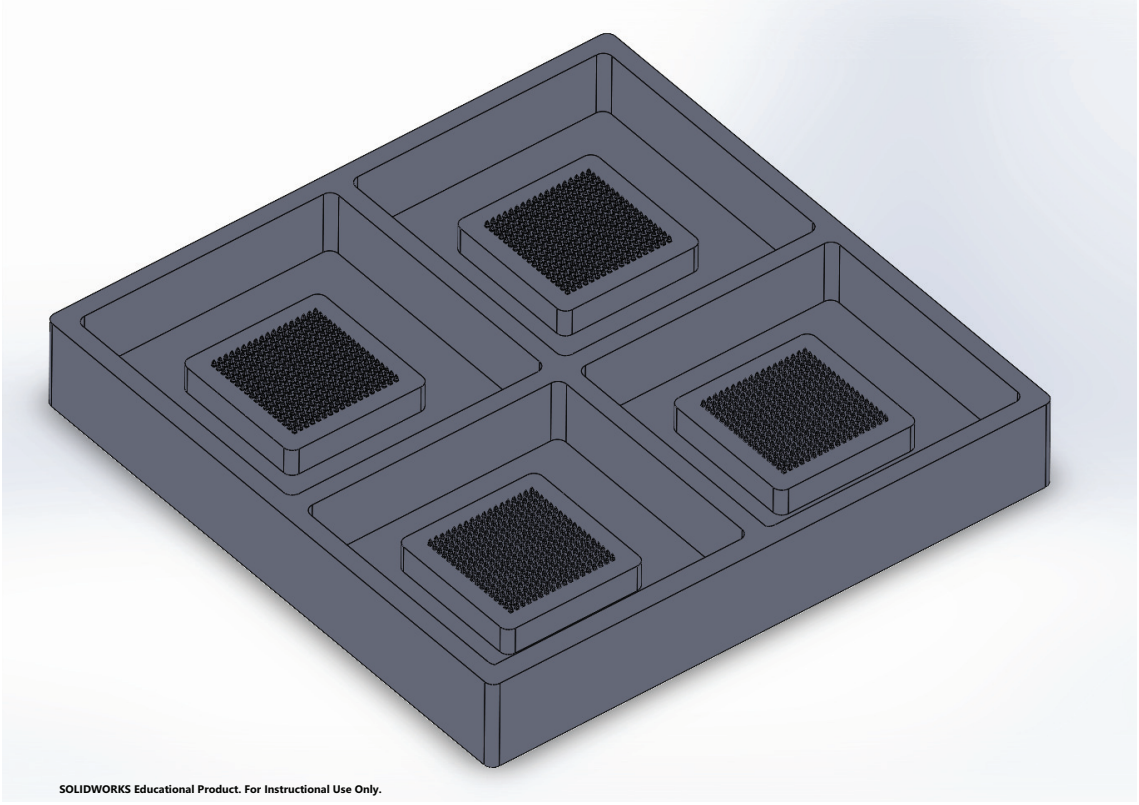

Figure 2.8: Master mold CAD model designed in SOLIDWORKS

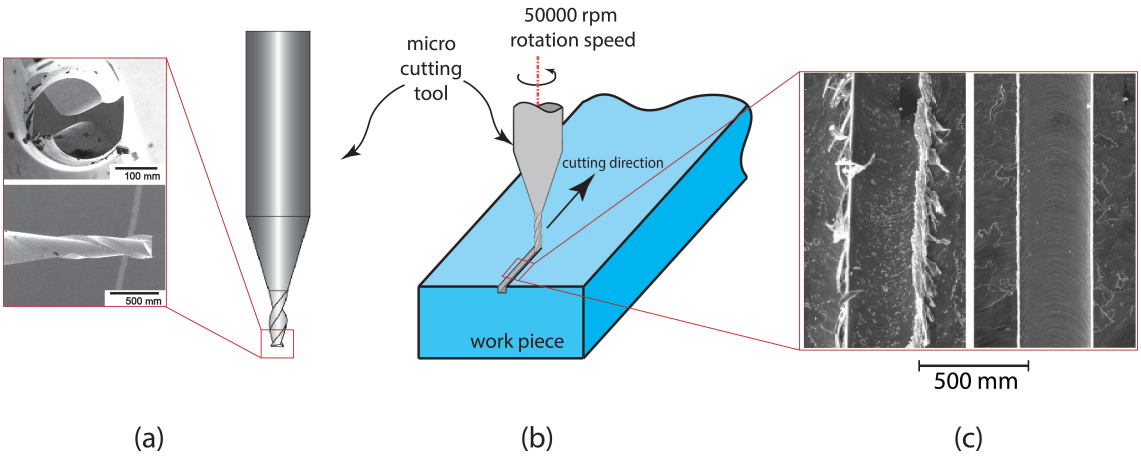

Figure 2.9: Production of master molds by micro milling.

The scanning electron microscopic (SEM) images illustrate an example of the manufactured master molds as a result of the presented fabrication process (Fig. 2.11). SEM-SE images of the microneedles were take the by using the Jeol JIB-4601F FIB-SEM System. It is observed from the images that the needles, both in arrays and individually, are obtained in their exact shapes and in the predicted sizes without any structural deterioration in their geometry and morphology. Note that

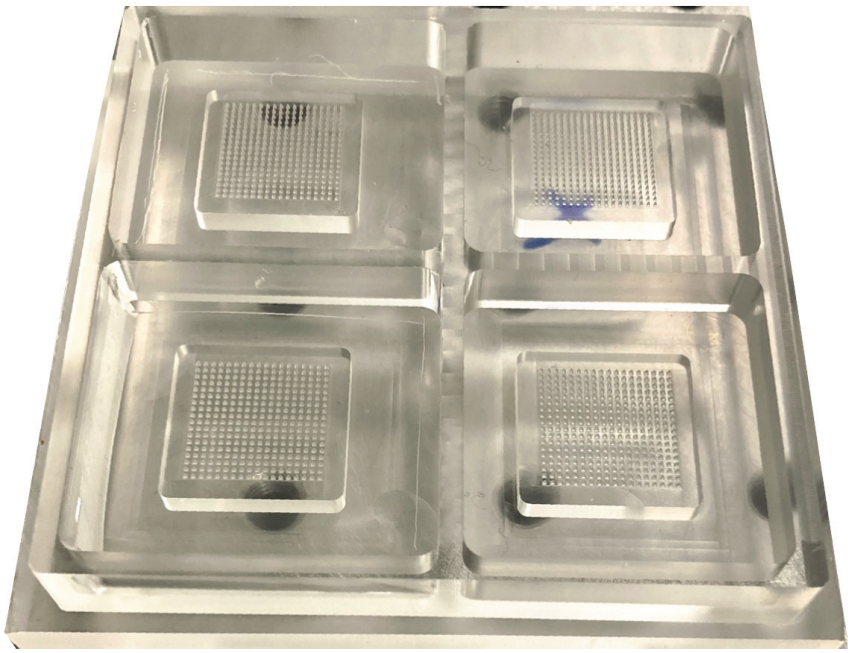

Figure 2.10: Fabricated master molds.

due to the tool-runout errors during the machining process, there is 5-8 % difference between the targeted and the final master molds. However, in determining the optimal dimensions from the Pareto-optimal set, we selected a conservative set where the safety factor is approximately 8.

2.4 Fabrication of Production Molds

As micro-casting is the primary method for fabricating MNAs, the next step in the process is to fabricate the production (female) molds. The material used in the production molds is Polydimethylsiloxane (PDMS) which is purchased from Sylgard®. PDMS, is a type of silicone which is from a group of organic polymer materials. It is one of the commonly used silicon based materials, due to its unique properties and characteristics that make it suitable for a wide range of applications from contact lenses to various pharmaceutical devices [100]. The production molds are fabricated by the following steps:

- The PDMS is mixed with the corresponding curing agent at a weight ratio of 10:1.

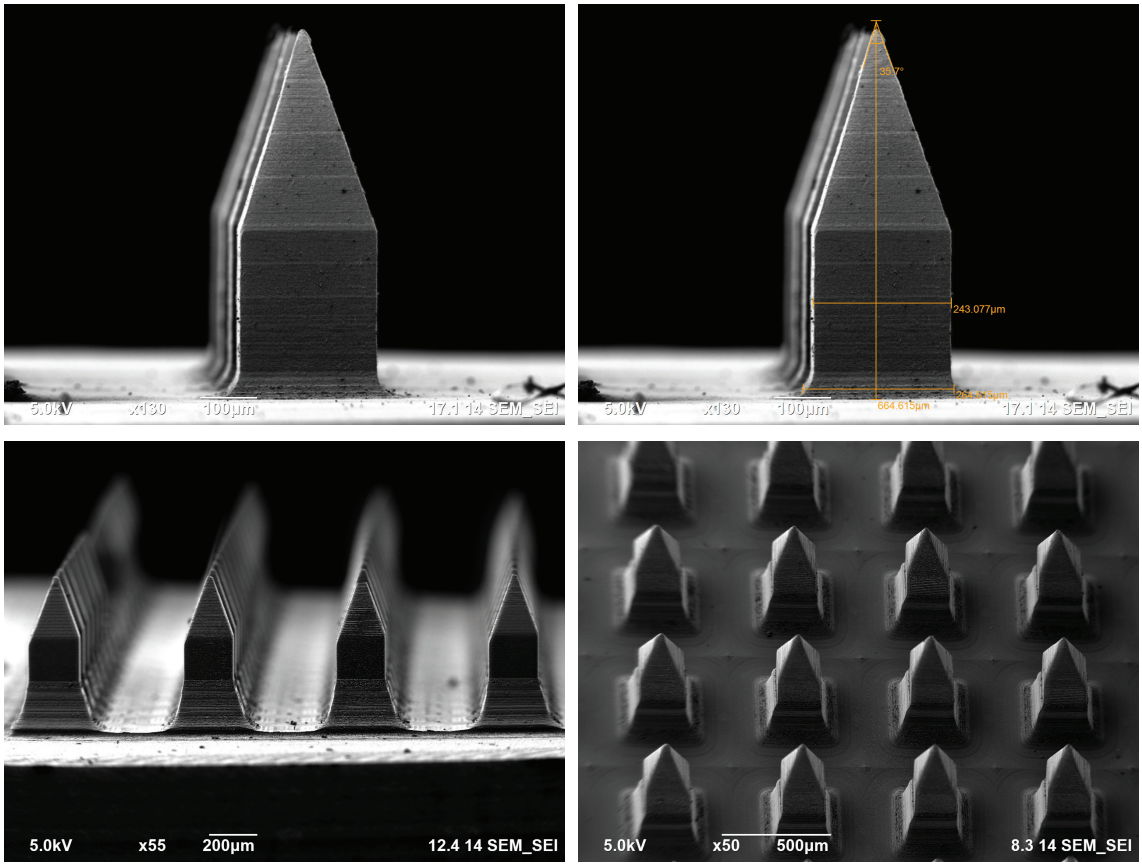

Figure 2.11: Scanning electron microscopy images of the fabricated master molds and their characterization.

- Ensure that the PDMS and curing agent are mixed thoroughly to avoid air bubbles/microbubbles.
- To remove any air bubbles that may have been generated, place the mixture under vacuum inside a desiccator for at least 10 minutes then break the vacuum.
- Repeat the vacuuming cycle multiple times to eliminate or minimize the generated microbubbles.
- Once the bubble-free mixture is ready for molding, it is poured into the master mold to form a layer of approximately $10mm$
- The vacuuming cycle is repeated multiple times to eliminate or minimize the generated microbubbles.
- Next, the master mold is placed in the oven and cured for 1 hour at $75°C$.
- After the cured molds cool at room temperature, they are separated from the

main mold with the help of scalpel and tweezers.

A step-by-step process of fabricating the production molds with the prepared PDMS mixture is shown in Fig. 2.12 along with the fabricated production mold and its cross section illustrated in Fig. 2.13.

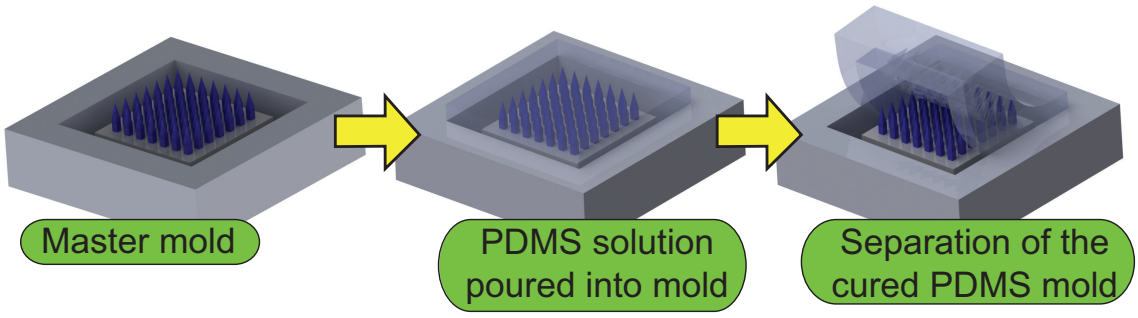

Figure 2.12: Fabrication of microneedle production molds using PDMS material.

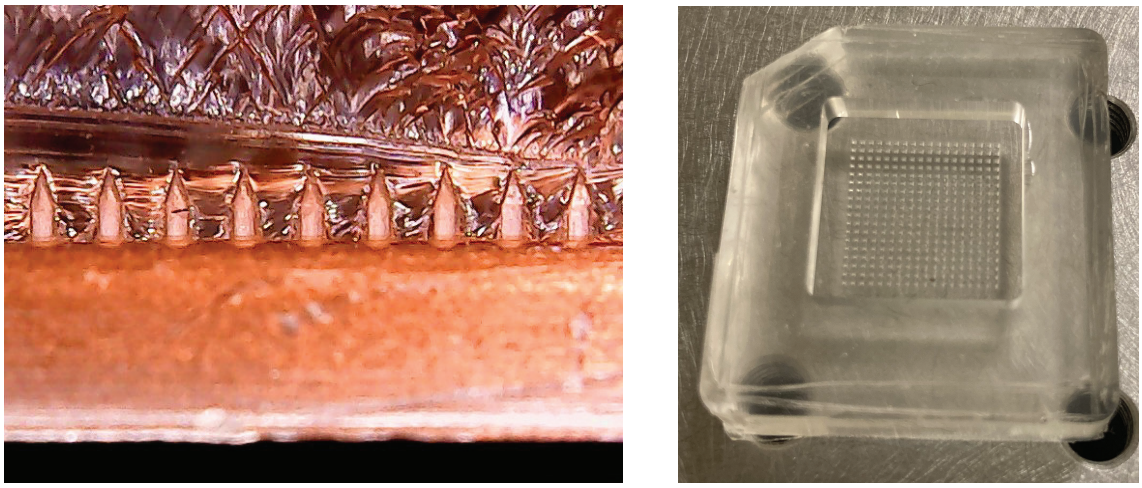

Figure 2.13: Fabricated production mold and cross section illustrating the microneedle cavities.

2.5 Preparation of Hydrogel

By aiming to fabricate dissolving MNAs, the material set out to be utilized must have specific properties and qualities. Taking into consideration that the material will be applied to human skin, it should be (i) biodegradable; which means that the material must be capable of dissolving under the skin of a human or living being, and (ii) it should be biocompatible; meaning that the material should not have any toxic or immunological response when exposed to the body.

The cartilage is tissue which is mainly consisted of various components such as GAGs, HA and CS, where they typically form the proteoglycans found in cartilage when linked to protein chains. Combining GAG, CS, and HA can be used to engineer cartilage tissue as substitutes for the extracellular matrix. On the contrary, they lack good mechanical properties, as do most natural polymers. Water-soluble synthetic polymers, such as PEGs, are usually used for creating bio-mimetic hydrogels with enhanced mechanical characteristics [101].

Accordingly, polymers such as GAG, CS, HA, PVP and PEG 400 are used for preparing the hydrogel solutions. The hydrogel solution is prepared with certain ratios of the stated material. The ratios are calculated and measured with considering the dosage of each patch, volume of each needle and material properties of each ingredient, such that the viscosity of the solution is suitable for casting. This would allow the mixture to easily enter and fill the needle cavities of the production molds. For the purpose of drug delivery, according to our specified application, the hydrogel consuming bioactive materials are used for tip loading, where a certain amount of Red Congo dye was added to the solution to monitor and trace the regions of the bioactive substances in the needle. Table 2.4 shows the formula and composition for different formulated patch types, with two main dosages, 1.2 mg and 2 mg of bioactive material in each patch.

Table 2.4: Composition of MNAs containing 1.2 mg and 2 mg doses of bioactive material

Formula No.	GAG (mg)	HA (mg)	CS (mg)	PVP (μl)	PEG 400 (μl)	Water (μl)	Red Congo dye (μl)
1	1.2	-	-	0.83	0.17	5.2	5.2
2	-	1.2	-	0.83	0.17	5.2	5.2
3	-	-	1.2	0.83	0.17	5.2	5.2
4	0.6	0.6	-	0.83	0.17	5.2	5.2
5	-	0.6	0.6	0.83	0.17	5.2	5.2
6	0.6	-	0.6	0.83	0.17	5.2	5.2
7	2	-	-	0.83	0.17	4.7	4.7
8	-	2	-	0.83	0.17	4.7	4.7
9	-	-	2	0.83	0.17	4.7	4.7
10	1	1	-	0.83	0.17	4.7	4.7
11	-	1	1	0.83	0.17	4.7	4.7
12	1	-	1	0.83	0.17	4.7	4.7

Additionally, a separate hydrogel solution containing only PVP and PEG400 is used for preparing a backing layer for the MNAs. By dissolving 2.06 g of PVP and 0.1 g

of PEG 400 in 25 ml of Ethanol, the backing layer solution was prepared.

2.6 Fabrication of MNAs

When the micro-casting technique is carried out, in order for the hydrogel solution to fill the needle cavities after being poured onto the production molds, a force must be applied. Literature has presented many possible approaches, including the using centrifuges with spin-casting technique, where the solution can easily enter the pores [46]. As an alternative, vacuuming can also be used as an effective and fast way for the solution to be drawn into the needle cavities. The vacuuming process is also used to get rid of the trapped air microbubbles inside the solution.

The following steps are required for the fabrication of MNAs.

- After preparing each group of hydrogel solution, they are put for stirring for at least 24 hours so that a homogeneous solution can be obtained.
- The solution consisting bioactive material is initially poured onto the production molds for fabrication of tip-loaded MNs.
- The production molds containing hydrogel solution are put under vacuuming.
- The vacuuming cycle is repeated multiple times to ensure the solution has filled the the needle cavities.
- The production molds are left to dry for 24 hours inside an oven and since it contains bioactive molecules the temperature must not exceed over 30deg in order not to damage the bioactive substances.
- Once the initial layer is completely dried, the backing layer solution is then added as multiple layers with the same steps of vacuuming and drying.
- Ultimately after the patches are dried, they ready to be taken out of the production molds.

A step-by-step process of fabricating the MNA patches is shown in Fig. 2.14.

2.7 Characterization of MNAs

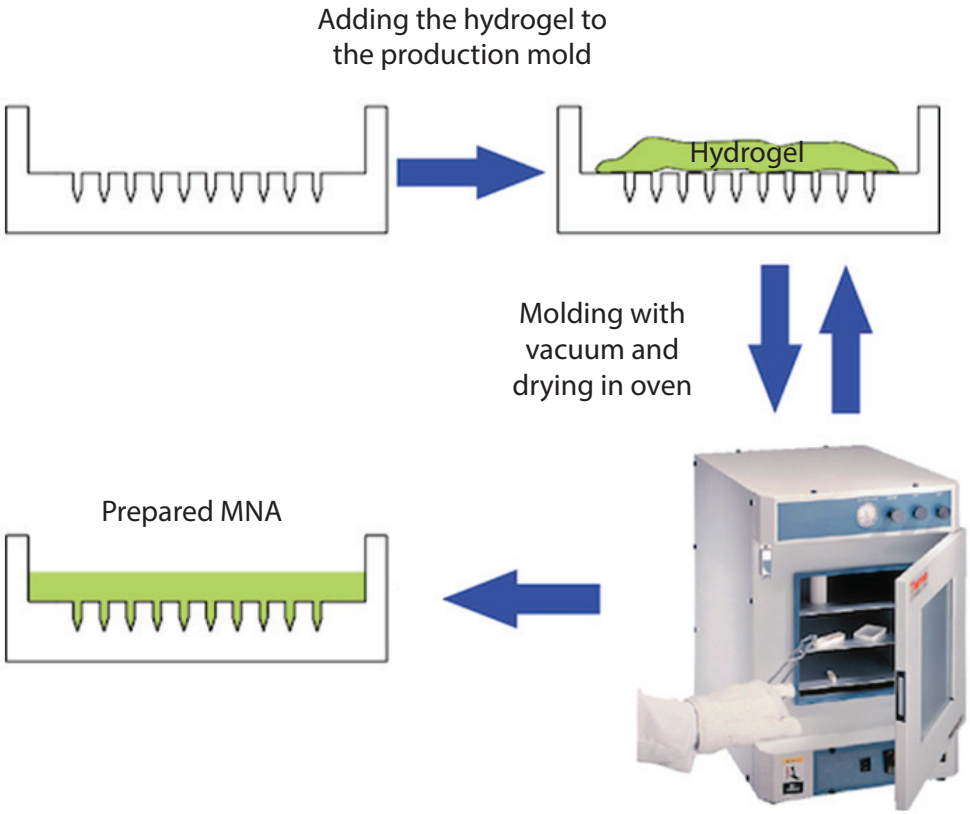

Figure 2.14: Step-by-step fabrication process of MNAs.

The fabricated MNAs and their geometry dimensions are characterized using an optical microscope. Figures 2.15 and 2.16 illustrates the final MNA patches. Images indicate that the needles, either in arrays or individually, retain their exact geometry and morphology without structural deterioration. It should be mentioned that due to the shrinkage of the fabricated MNA, as a result of the drying process, there is a 0.75-0.80 % difference between the master molds needle dimensions and the final MNAs. In conclusion, micro-casting technique is an effective method for rapidly producing MNAs in a variety of materials and geometries.

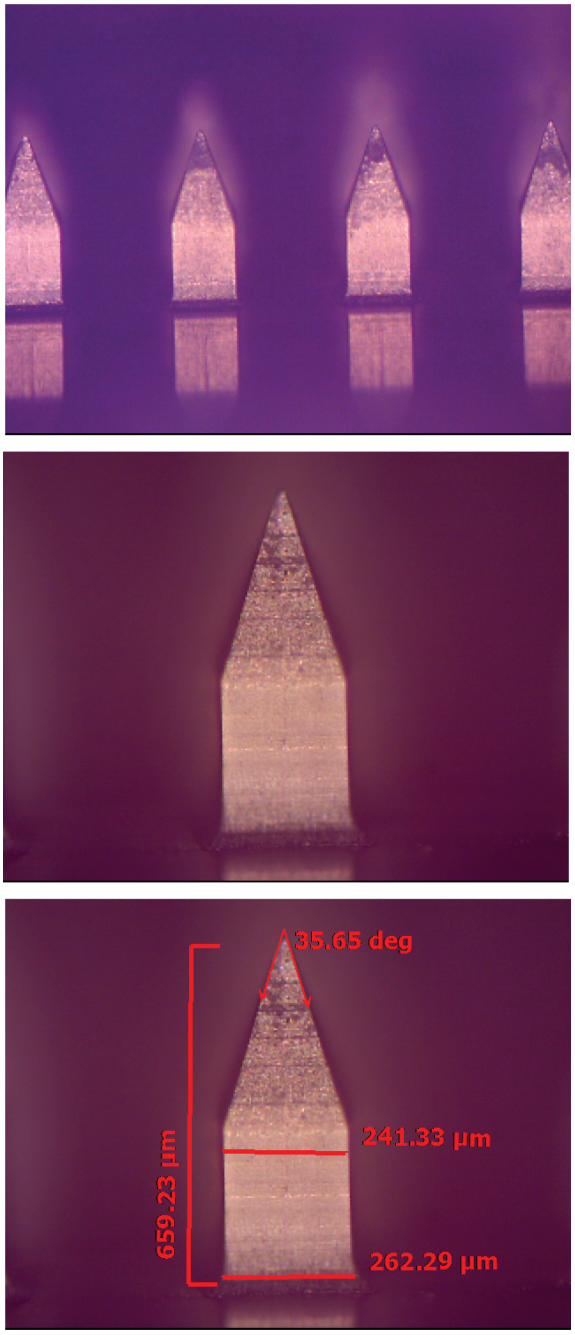

Figure 2.15: Optical microscope images of the fabricated MNAs and their characterization

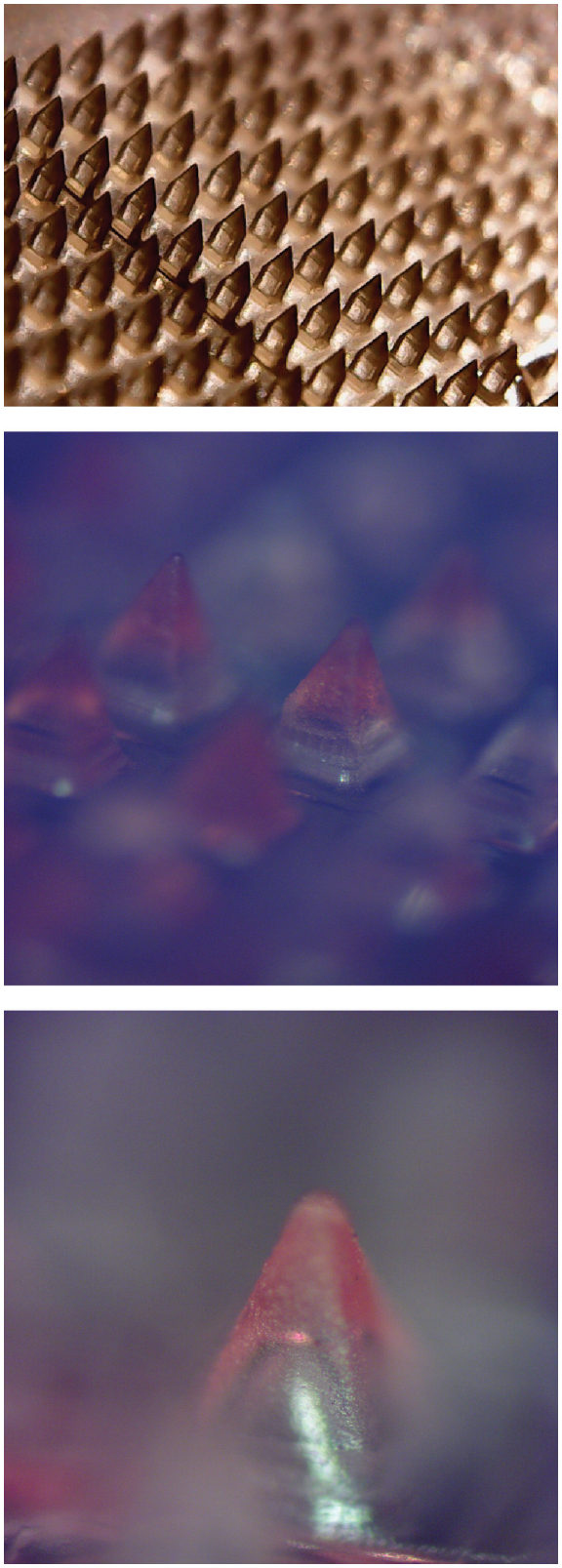

Figure 2.16: MNA patch and tiploaded with biocargo microneedles

Chapter 3

In-Vitro Tests

Following the fabrication of MNAs which contain bioactive cargo with their optimal geometry, a variety of in-vitro tests were performed to evaluate their performance and abilities:

- Their mechanical feasibility in piercing the skin
- Dissolving time rate
- Determining dosage amount of each patch
- Ability of wound-healing
- Cell viability
- Cytotoxic effects of the bioactive cargos contained in each patch

Throughout the following sections, the methodology and details of each test that was performed have been discussed, including the piercing, dissolution, HPLC, scratch assay, proliferation and cytotoxicity tests.

3.1 Piercing test

Researchers have demonstrated that the skin has a hyperelastic behavior, and that the elastic behavior is higher than when a light force is exerted [102]. Microneedle geometry plays a crucial role in achieving efficient insertion into the skin. Therefore, to test the ability of the manufactured and optimized MNs in penetrating the skin, in-vitro piercing test is performed. To this end, an artificial gelatine-based skin sample was prepared with a thickness of 0.13 mm, as a surrogate for representing the human skin environment. The skin sample is fabricated following the study of

Dabrowska et al. [103]. Due to the fact that using the artificial skin sample alone does not accurately reflect the mechanical characteristics of human skin, a substitute must be developed to be used in conjunction with the gelatine-based skin sample. Therefore, in addition to the artificial skin sample, PDMS can be used as a suitable elastic medium for mimicking the underneath supporting subcutaneous tissues of the skin based on previous research [102].

To carry out the penetration test, microneedle patches are inserted into the skin sample with the force of hand, which are stretched and supported by PDMS medium. The result of penetration is observed investigated by microscopic images shown in Fig. 3.1. It can be seen that the fabricated MNAs create micro-pores within the skin and are able to successfully penetrate the skin sample without any defects and breaking.

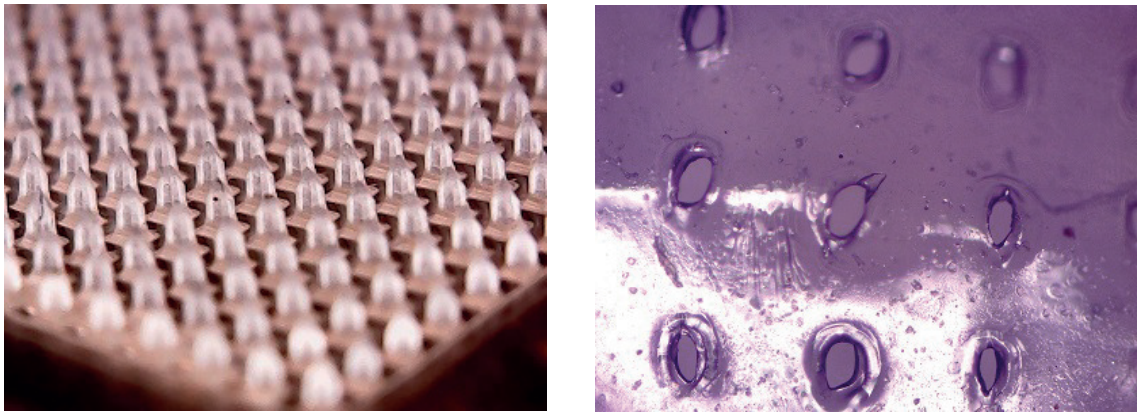

Figure 3.1: Microscopic images showing the in-vitro piercing test results: (a) microneedle array, and (b) pierced artificial skin.

3.2 Dissolution Test

It is important to take into consideration when fabricating MNAs, the materials used for production must have the ability of rapidly dissolving inside the human skin environment. A dissolution study is carried out to estimate the time rate at which the microneedles can dissolve in the skin and release their bioactive load. A short dissolution time is considered best and more suitable for the applicability of MNAs.

For this purpose, a soluble solution of Phosphate-Buffered Saline 10x (10xPBS) and distilled water with a weight ratio of 1:9 is prepared to simulate skin as a solvent. In this test, four groups of MNAs are examined, including formulas 1, 3 and 6 from Table 2.4 and an additional control group with the composition of the backing layer which only included PVP and PEG400. For dissolution analysis, by using a linear actuator with micrometer advancement capacity, the fabricated MNAs are gently immersed in the prepared PBS solution. The process is observed and monitored with the help of an optical microscope in order to observe the dissolved portions of the needle. The lab setup to carry out this test can be seen in Fig. 3.2.

The tests reveal that the MNs dissolved within 10 seconds after having contact with the solution, and a noticeable decrease in size is observed in the needles. Figure 3.3 shows the MN geometries at 3.6, 5 and 10 seconds. The entire microneedle geometry is also completely dissolved after 10 seconds of contact with the PBS solvent. This indicates that a relatively short period of use is sufficient for the dissolution of microneedles and to release the bioactive material in the skin. Instant solubility is an important feature of this drug delivery system as it improves the patients compliance and satisfactory level.

3.3 HPLC Method

As part of the design and fabrication process of the MNAs, the ability of the structure to contain and release the appropriate level of bioactive substance for the purpose of drug delivery is an important factor to take into account. To accomplish this, a test was conducted to find the dosage amount and to determine whether the desired concentration could be placed in each microneedle patch. This was accomplished by using the high performance liquid chromatography (HPLC) method. HPLC is an an-

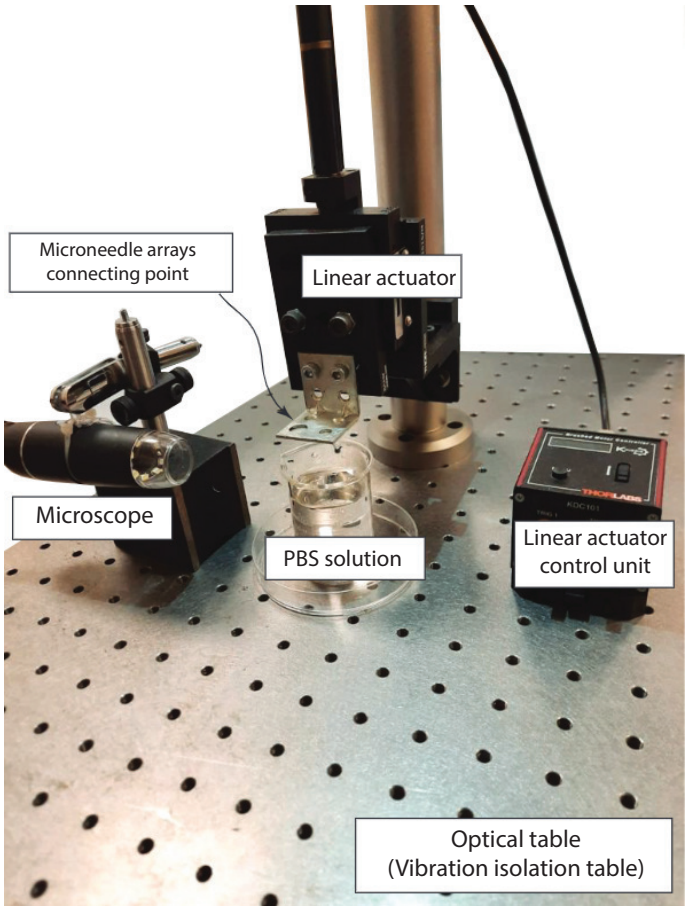

Figure 3.2: Lab setup of the dissolution test

alytical method that is capable of quantifying, separating, and detecting impurities in a substance, as well as drug degradation that may occur during its preparation or storage. The development of this method is facilitated by understanding the chemistry of the active substance. Support was received from Nobel Pharmaceutical Company for these analyses. Since these measurements work with very small doses, unlike in literature, a new procedure was created by the company and measurements were carried out. The test methodology is simply shown in Fig. 3.4.

For this test, seven different MNA samples containing bioactive materials (Formulas 1, 3, 6, 7, 9, and 12) and a control group (MNAs without bioactive material) in the amounts specified in Table 2.4 were produced with two different amounts of dosage (1.2 mg and 2 mg). In this procedure, samples were placed in a 100ml measuring flask and dissolved in 20ml of diluent. It was sonicated for approximately 10 minutes and then the volume was made up with diluent. In the last step, the solution was filtered through a 0.45 μm PTFE filter.

In Table 3.1, the results and amounts of bioactive material in each microneedle patch

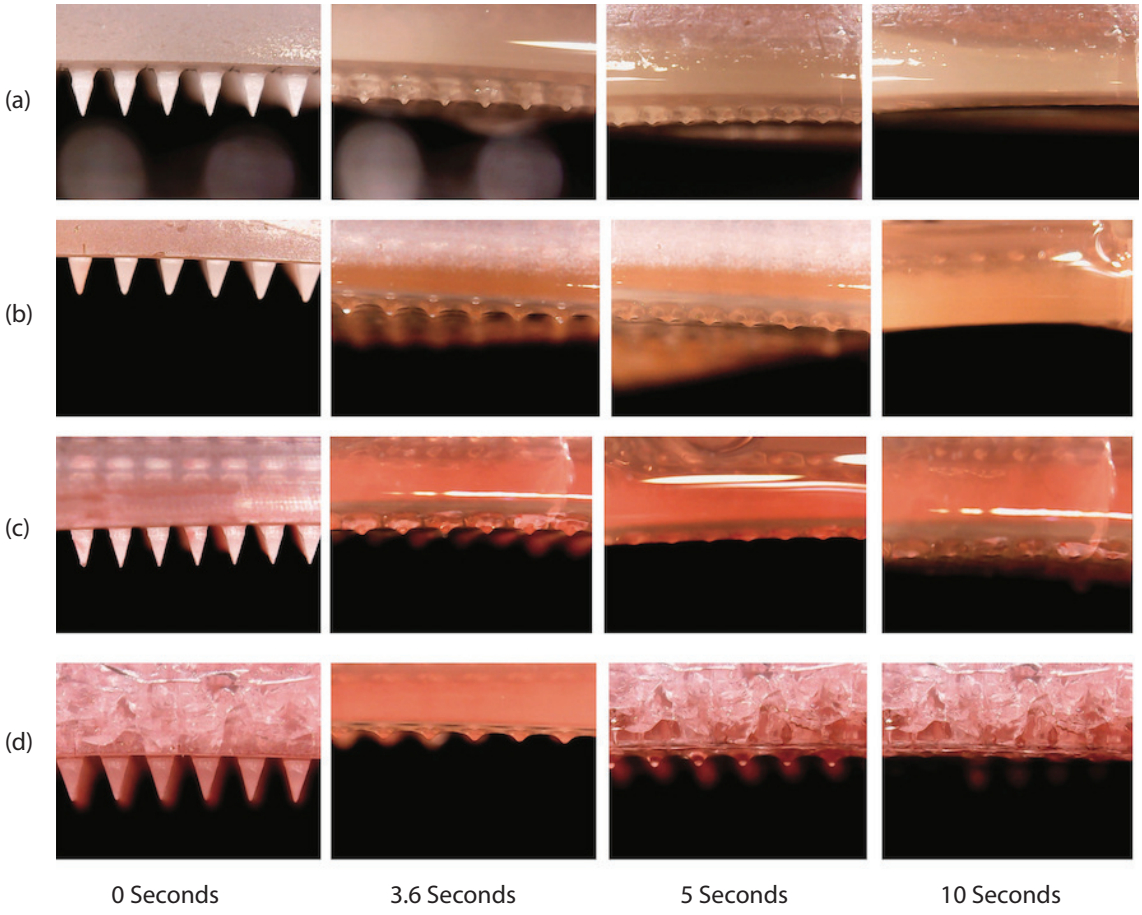

Figure 3.3: Microneedle dissolution tests, illustrating the results for (a) Control group (PVP+PEG400), (b) Formula 1, (c) Formula 3, and (d) Formula 6.

used in the tests are indicated. It was stated by the company that the amount of error in the measurements was 0.5 mg. According to Table 3.1, the production methodology does not disrupt the biomaterial structure and the dosage amount can be controlled successfully. Nevertheless, further studies are needed to adjust the amount of biomaterial more precisely and to determine the dose amount for clinical studies.

3.4 Proliferation and Cytotoxicity Test

Numerous in-vitro tests investigating the reaction of a cell population to environmental factors are based on the measurement of cell viability and proliferation. The MTT assay is a colorimetric assay for understanding cell proliferation, viability and cytotoxicity of substance. This assay is based on the ability of NADPH-dependent

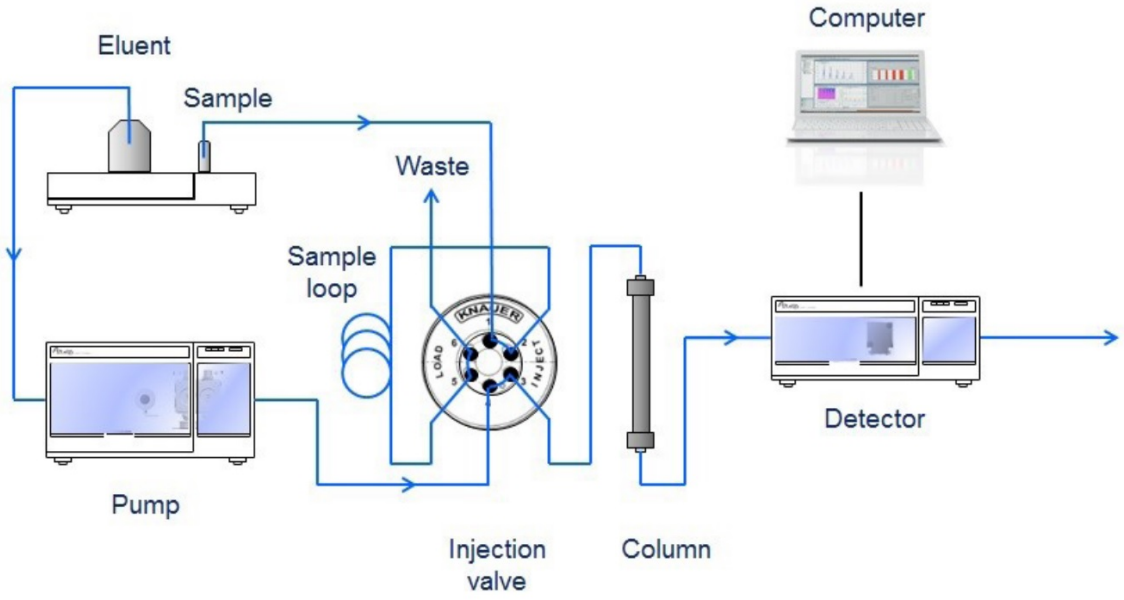

Figure 3.4: Schematic layout of an HPLC system [4]

Table 3.1: Drug dosage test using the HPLC method results

	CS		GAG		CS + GAG				Control Group
	mg	mg	mg	mg	CS mg	GAG mg	CS mg	GAG mg	mg
Target dosage	1.2	2	1.2	2	0.6	0.6	1	1	0
Test 1	1.56	0.91	1.16	1.95	0.48	0.63	0.96	1.15	ND
Test 2	0.55	2.11	0.97	1.92	0.38	0.46	0.82	1.10	ND
Test 3	1.27	1.47	1.20	2.07	0.24	0.56	0.66	1.08	ND
Average	1.13	1.50	1.11	1.98	0.37	0.55	0.81	1.11	-
S.D.	0.52	0.60	0.12	0.08	0.12	0.08	0.15	0.04	-
Performance	% 72	% 75	% 93	% 100	% 62	% 92	% 81	% 100	-

cellular enzyme to reduce the Tetrazolium dye (MTT) to its insoluble Formazan format. MTT is a Tetrazolium salt which is yellowish in color, and can be reduced to Formazan format which is violet in color. This color change is only possible when the cell is viable [104]. Therefor, using this principle MTT profileration and cytotoxcity assay is performed.

For the proliferation analysis, human chondrocyte cells and osteoblast cells were seeded in a 96-well culture dish and incubated with growth media at 37°C and 5% CO2 conditions until they reached 70% density. The sample material was incubated at the same conditions in the first, third and seventh days. 10 μl of MTT solution

was added to each well and incubated for two hours , and absorbance values were obtained in the ELISA reader at 570 nm wavelength of the culture dish. The experiment was carried out in four repetitions.

For the cytotoxicity test; L929 mouse fibroblast cells were seeded in a 96-well culture dish and incubated with their medium at 37°C and 5% CO2 until they reached 80% density. Afterwards, incubation was carried out with the sample material in the first, third and seventh days. 10 μl of MTT solution was added to each well and incubated for two hours, and absorbance values were obtained in an ELISA reader at 570 nm wavelength of the culture dish. The experiment was carried out in four repetitions.

Considering the proliferation analysis as shown in Fig.3.5, no significant difference in both hFOB and HC cell lines on the first day is seen, but it is observed that both cell lines increased significantly compared to the other groups with complex material. It has been observed that the materials affect cell proliferation synergistically. In the cytotoxicity analysis, on the first day there was no difference between the groups, but the complex material increased significantly on the 3rd and 7th days compared to all groups. As a result of the evaluations, it was observed that the materials did not have any cytotoxic effect.

3.5 In-vitro Scratch Assay

To estimate the ability of the bioactive material which are released into the skin to heal wounds, scratch assay is performed. Cellular migration is a critical wound healing process that can drastically alter the outcome of a healing wound. This protocol allows researchers to better understand the effect of compounds in cellular migration during wound healing. The scratch assay is a cost effective and high-throughput approach for generating meaningful wound healing data prior to costly and time-intensive in-vivo testing [105, 106].

To carry out this test, human chondrocytes are seeded in a 6-well culture dish and incubated at 37°C and 5% CO2. When the cells reach 90% density, scraping is performed with a 100 ml sterile pipette. Cell debris are removed by rinsing with PBS and microscopy imaging is performed at 10x magnification. At the 24th and 48th hours of the experiment, photographs of the scraped area are taken and comparisons and measurements are made with Image-J software. The experiment is carried out in three repetitions.

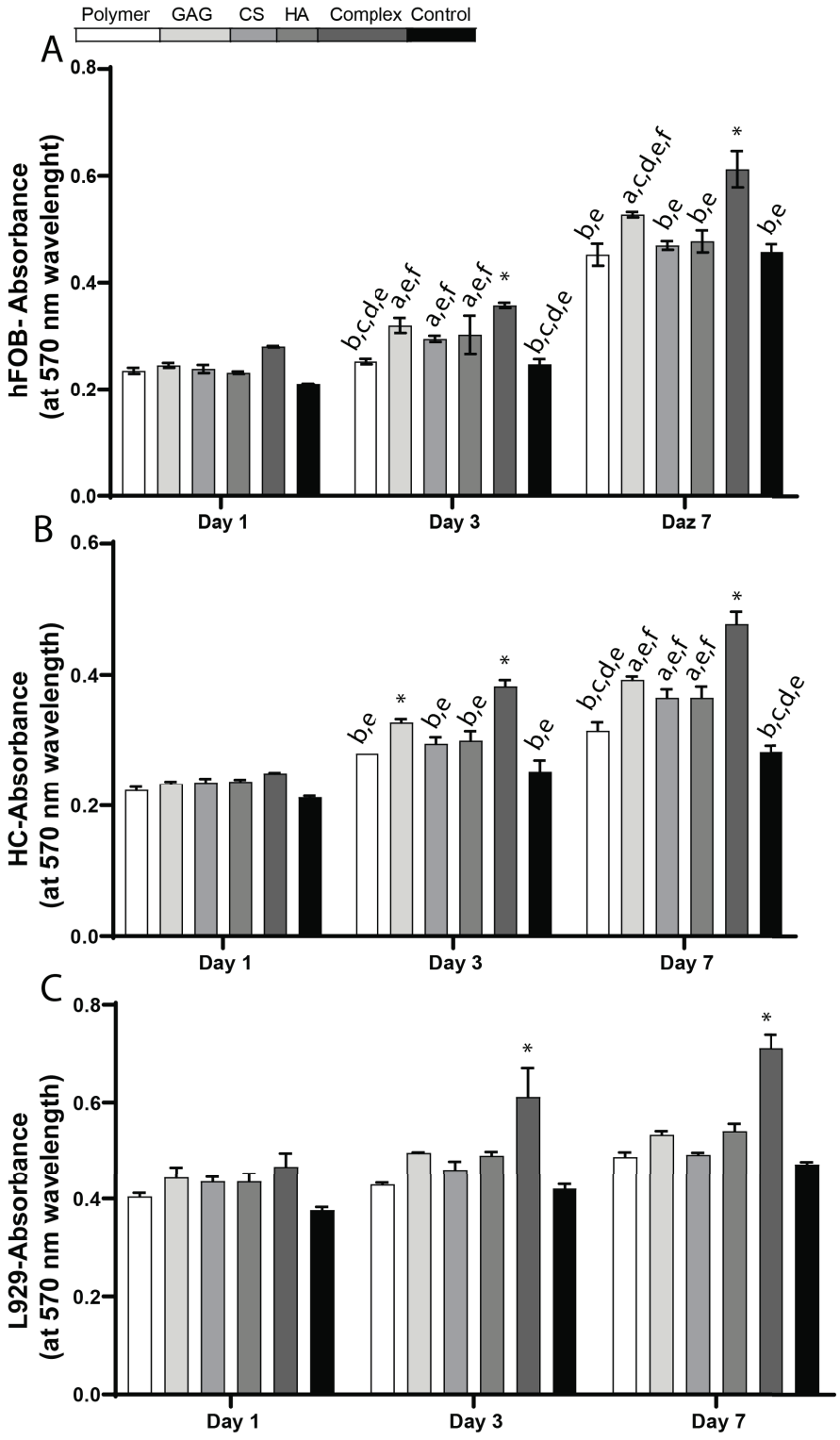

Figure 3.5: Bar graph of the proliferative effect of the complex material on (A) hFOB, (B) HC and (C) cytotoxic effect on L929 fibroblast cell line. $p<0.05$ shows $p<0.05$ compared to (a) polymer, (b) GAG, (c) CS, (d) HA, (e) complex and (f) control.

As a means of simulating wound-healing in the human body, the effect of bioactive materials on the wound healing procedure has been assessed with the scratch assay, followed by monitoring the cellular response.

In the morphological evaluation, there was no difference between the groups on Day 0, but the density of the GAG and complex groups increased rapidly on Day 1. In the second evaluation, although closure increased in all groups, the scraping line could not be noticed only in the group containing complex material. Significant void areas were observed in the control group and polymer group, where no material was applied. The results of the scratch assay regarding each group of MNAs are illustrated in Fig.3.7, showing the migration of cells in detail. Figure 3.6 shows the average cell amount as a result of the scratch assay. It can be concluded that the complex group which consists of a combination of bioactive materials such as GAG, CS and HA is the best-healed group by comparison.

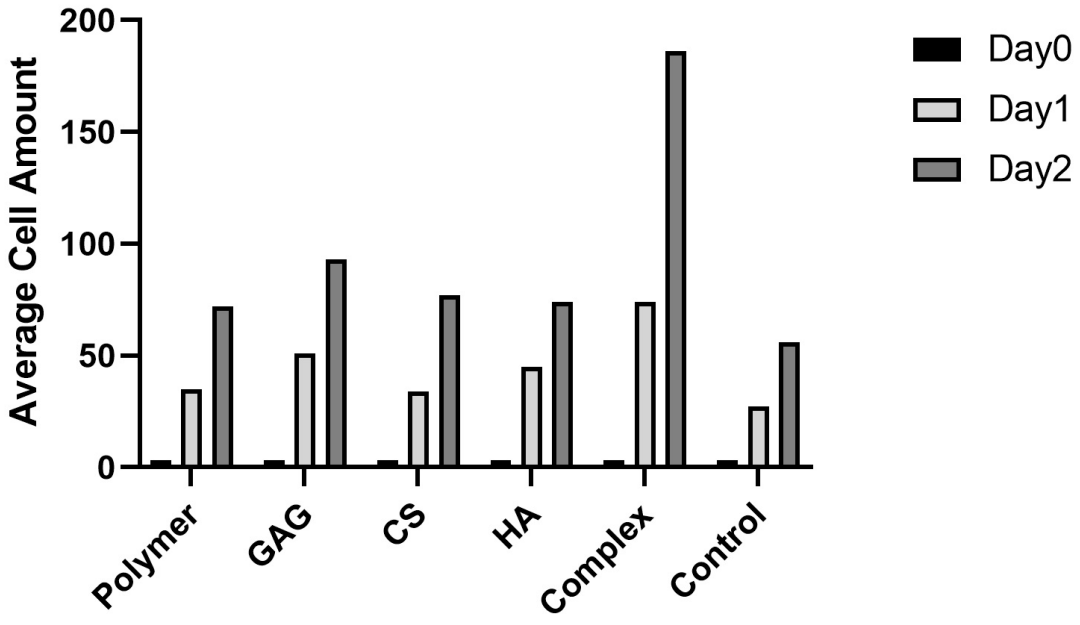

Figure 3.6: Scratch assay graph results, illustrating the average cell amount as a result of the cell migration after 0, 24 and 48 hours.

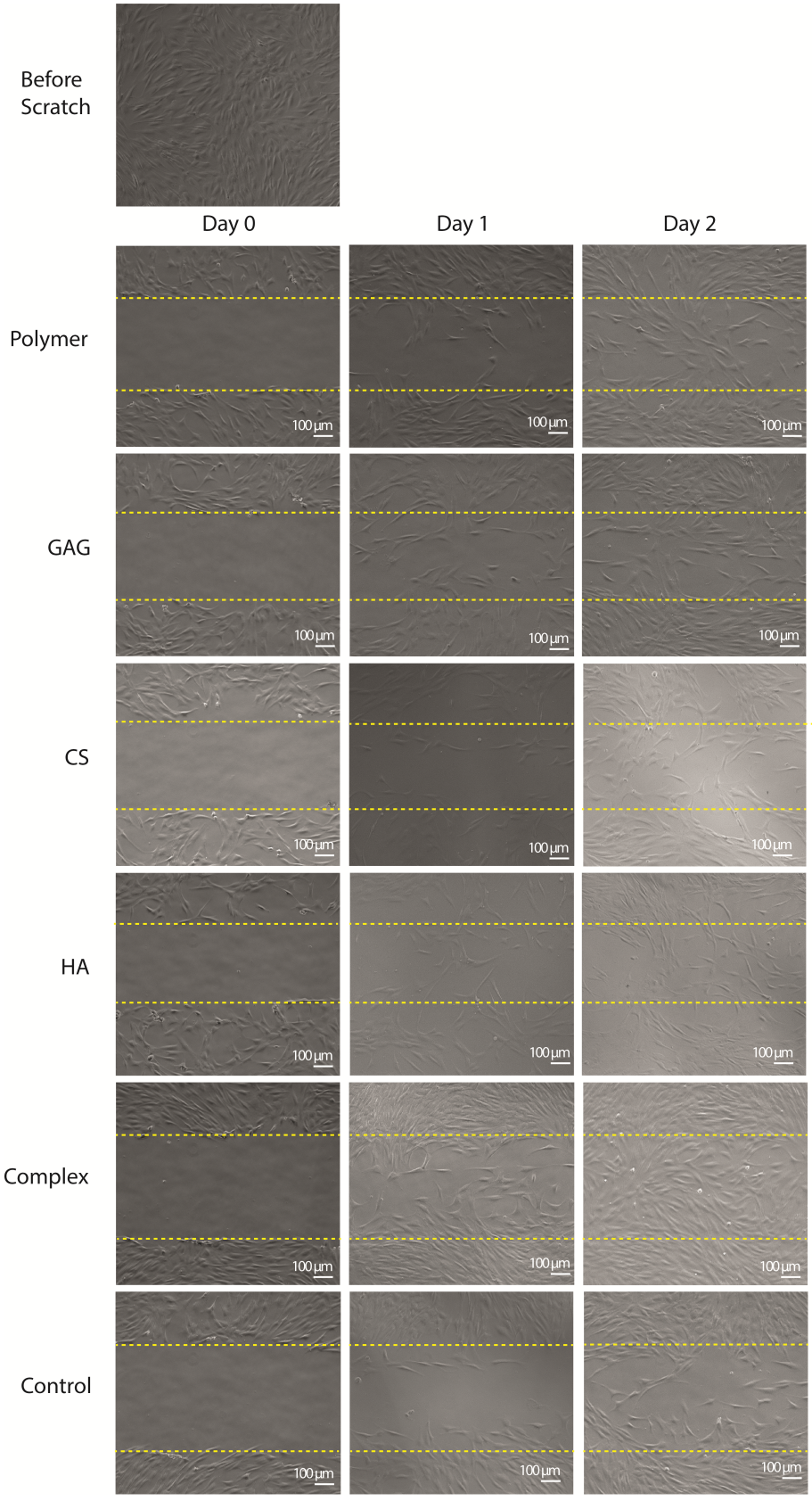

Figure 3.7: Micrographs of the effect of the composite material on wound healing on chondrocytes are seen. (10x) Yellow dashed lines indicate the wound area.

Chapter 4

Conclusion and Recommendations

4.1 Conclusions

In this study, a multi-objective optimization based on the NSGA-II is carried out to determine the optimal geometry of a microneedle geometry to prevent breakage during the insertion process. In order to perform the optimization, MATLAB and COMOSOL Multiphysics are linked together, and subsequently a reasonable safety factor is used to select the optimal dimensions of each model. Based on the optimal MN dimensions selected, master molds are fabricated using PMMA material by micro-milling technique. Then, with the aid of micro-molding technology, the PDMS production molds are produced. Consequently, dissolvable microneedle arrays are developed to cure Osteoarthritis disease. For this purpose, solutions containing polymers such as glucosaminoglycan, chondroitin, hyaluronic acid, poli(vinil pirolidon), and poli(etilen glikol) are made such that the microneedles function properly. The geometry of the master molds and final MNAs are characterized by optical and scanning electron microscopy images which indicates the stated production process is capable of fabricating the MNAs with the desired dimensions. To verify the appropriate functioning, series of in-vitro tests including piercing, dissolution, HPLC, scratch assay, proliferation and cytotoxicity tests are performed. From the results of the tests conducted, it can be concluded that the microneedles have the following capabilities in terms of:

- Their ability to penetrate the skin without any defects and breaking.
- A relatively short period of use is sufficient for the microneedles to dissolve and release their bioactive material in the skin

- The production methodology does not disrupt the biomaterial structure and the dosage amount can be controlled successfully.
- The ability of wound-healing.
- The materials used in the fabrication of MNAs affect cell proliferation and viability synergistically.
- It was also found that the materials used in preparing MNAs did not cause any cytotoxicity to the cells.

It has also been concluded from these series of tests that the complex group, which is a combination of all of the polymers stated above, has the best results in comparison with the other polymers studied.

4.2 Recommendations

There are a few recommendations that can be made below in order to improve the development of future simulations and models:

- For interpreting a realistic model for the insertion and penetration of the microneedle arrays into the skin, developing simulations that can demonstrate the actual force which is applied from the skin to the microneedle and checking whether the needles have the ability to pierce the skin, it can be beneficial for obtaining more optimal dimensions for the square obelisk geometry before having to manufacture them.
- It has been stated that the skin has an hyperelastic behaviour. The skin can be modeled with various types of hyperelastic materials such as Neo-Hookean, Ogden, Mooney–Rivlin, and etc., that have different parameters. Experiments and tests can be performed for obtaining these parameters to better analyze the microneedle insertion to the skin.
- Depending on the application, some microneedle array patches are inserted to the skin by using applicators. Modelling the applied force during insertion along with the reaction force from the skin can assist predict the performance of the needle structure.
- When inserting a microneedle array patch into the skin, the needle spacing and total number of needles on a patch will effect the reaction force, which

may cause (i) failing to penetrate the skin (ii) breakage of the needles and (iii) discomfort during insertion. By developing simulations to determine the ideal dimensions, needle number, and spacing, needle feasibility, and patient compliance can be increased.

- For applications and drug delivery purposes, developing simulations where the drug release rate can be observed based on the materials and compounds utilized in the fabrication of microneedles can help predict the performance of the patches along with their relevant in-vitro tests.
- The use of new substances and compounds for the purpose of treating or addressing a wide variety of medical problems.
- In the present day, various diseases and viruses can cause pandemics, such as the one that we are currently experiencing. Since today's vaccinations have certain limitations when facing pandemics, such as storage, production on a global scale, generating bio-hazardous waste. Microneedle arrays can be considered the future of vaccinations by developing new and unique shapes, geometries, fabrication methods, and application strategies for the purpose of mass production.

Bibliography

[1] L. Ventrelli, L. Marsilio Strambini, and G. Barillaro, "Microneedles for transdermal biosensing: current picture and future direction," *Advanced healthcare materials*, vol. 4, no. 17, pp. 2606–2640, 2015.

[2] R. Nagarkar, M. Singh, H. X. Nguyen, and S. Jonnalagadda, "A review of recent advances in microneedle technology for transdermal drug delivery," *Journal of Drug Delivery Science and Technology*, vol. 59, p. 101923, 2020.

[3] P. Makvandi, M. Kirkby, A. R. Hutton, M. Shabani, C. K. Yiu, Z. Baghbantaraghdari, R. Jamaledin, M. Carlotti, B. Mazzolai, V. Mattoli, *et al.*, "Engineering microneedle patches for improved penetration: analysis, skin models and factors affecting needle insertion," *Nano-Micro Letters*, vol. 13, no. 1, pp. 1–41, 2021.

[4] J. BÖTTCHER, M. MARGRAF, and K. MONKS, "Hplc basics–principles and parameters," *Science Together, KNAUER Wissenschaftliche Geräte GmbH*, 2019.

[5] R. M. Mainardes and L. P. Silva, "Drug delivery systems: past, present, and future," *Current drug targets*, vol. 5, no. 5, pp. 449–455, 2004.

[6] H. Reza Rezaie, M. Esnaashary, A. Öchsner, *et al.*, "The history of drug delivery systems," in *A Review of Biomaterials and Their Applications in Drug Delivery*, pp. 1–8, Springer, 2018.

[7] H. Park, A. Otte, and K. Park, "Evolution of drug delivery systems: From 1950 to 2020 and beyond," *Journal of Controlled Release*, vol. 342, pp. 53–65, 2022.

[8] Y. W. Chien, "Novel drug delivery systems," *Drugs and the pharmaceutical sciences*, vol. 50, 1992.

[9] A. M. Vargason, A. C. Anselmo, and S. Mitragotri, "The evolution of commercial drug delivery technologies," *Nature biomedical engineering*, vol. 5, no. 9, pp. 951–967, 2021.

[10] R. Langer, "Drug delivery and targeting.," *Nature*, vol. 392, no. 6679 Suppl, pp. 5–10, 1998.

[11] B. M. Rayaprolu, J. J. Strawser, and G. Anyarambhatla, "Excipients in parenteral formulations: selection considerations and effective utilization with small molecules and biologics," *Drug development and industrial pharmacy*, vol. 44, no. 10, pp. 1565–1571, 2018.

[12] K. K. Jain, "Drug delivery systems-an overview," *Drug delivery systems*, pp. 1–50, 2008.

[13] G. Tiwari, R. Tiwari, B. Sriwastawa, L. Bhati, S. Pandey, P. Pandey, and S. K. Bannerjee, "Drug delivery systems: An updated review," *International journal of pharmaceutical investigation*, vol. 2, no. 1, p. 2, 2012.

[14] R. K. Tekade, *Basic fundamentals of drug delivery*. Academic Press, 2018.

[15] T. M. Allen and P. R. Cullis, "Drug delivery systems: entering the mainstream," *Science*, vol. 303, no. 5665, pp. 1818–1822, 2004.

[16] L. Sanders, "Drug delivery systems and routes of administration of peptide and protein drugs," *European journal of drug metabolism and pharmacokinetics*, vol. 15, no. 2, pp. 95–102, 1990.

[17] H. Gupta, D. Bhandari, and A. Sharma, "Recent trends in oral drug delivery: a review," *Recent patents on drug delivery & formulation*, vol. 3, no. 2, pp. 162–173, 2009.

[18] A. Fasano, "Novel approaches for oral delivery of macromolecules," *Journal of pharmaceutical sciences*, vol. 87, no. 11, pp. 1351–1356, 1998.

[19] V. H. Li, J. R. Robinson, and V. Lee, "Influence of drug properties and routes of drug administration on the design of sustained and controlled release systems," *Controlled Drug Delivery*, vol. 29, no. 2, pp. 4–94, 1987.

[20] B. Homayun, X. Lin, and H.-J. Choi, "Challenges and recent progress in oral drug delivery systems for biopharmaceuticals," *Pharmaceutics*, vol. 11, no. 3, p. 129, 2019.

[21] E. Moroz, S. Matoori, and J.-C. Leroux, "Oral delivery of macromolecular drugs: Where we are after almost 100 years of attempts," *Advanced drug delivery reviews*, vol. 101, pp. 108–121, 2016.

[22] S. V. Sastry, J. R. Nyshadham, and J. A. Fix, "Recent technological advances in oral drug delivery–a review," *Pharmaceutical science & technology today*, vol. 3, no. 4, pp. 138–145, 2000.

[23] M. Groves, "Parenteral drug delivery systems," *Encyclopedia of controlled drug delivery*, vol. 1, pp. 743–777, 1999.

[24] K. Lippincott, "Williams. remington, the science & practice of pharmacy, parenteral preparation, volume," 2000.

[25] P. Verma, A. Thakur, K. Deshmukh, A. Jha, and S. Verma, "Routes of drug administration," *International Journal of Pharmaceutical Studies and Research*, vol. 1, no. 1, pp. 54–59, 2010.

[26] M. R. Prausnitz and R. Langer, "Transdermal drug delivery," *Nature biotechnology*, vol. 26, no. 11, pp. 1261–1268, 2008.

[27] L. Allen and H. C. Ansel, *Ansel's pharmaceutical dosage forms and drug delivery systems*. Lippincott Williams & Wilkins, 2013.

[28] K. Singh, N. Arora, and T. Garg, "Superbug: antimicrobial resistance due to ndm-1," *Int J Inst Pharm Life Sci*, vol. 2, no. 2, pp. 58–66, 2012.

[29] L. S. Nair and C. T. Laurencin, "Biodegradable polymers as biomaterials," *Progress in polymer science*, vol. 32, no. 8-9, pp. 762–798, 2007.

[30] N. Dragicevic and H. Maibach, "Combined use of nanocarriers and physical methods for percutaneous penetration enhancement," *Advanced drug delivery reviews*, vol. 127, pp. 58–84, 2018.

[31] M.-T. Nguyen, C.-I. Wu, J.-Y. Siao, Y.-Y. Hong, Y.-R. Chang, Y.-D. Lee, and S.-S. Wang, "Study on ufls strategy in a stand-alone power system," in *2018 4th International Conference on Green Technology and Sustainable Development (GTSD)*, pp. 68–71, IEEE, 2018.

[32] T. Klemsdal, K. Gjesdal, and J.-E. Bredesen, "Heating and cooling of the nitroglycerin patch application area modify the plasma level of nitroglycerin," *European journal of clinical pharmacology*, vol. 43, no. 6, pp. 625–628, 1992.

[33] A. K. Banga, "Foreword to transdermal delivery mini focus issue," *Therapeutic Delivery*, vol. 3, no. 3, pp. 293–294, 2012.

[34] S. N. Murthy, "Magnetophoresis: an approach to enhance transdermal drug diffusion.," *Die Pharmazie*, vol. 54, no. 5, pp. 377–379, 1999.

[35] J. Kost, U. Pliquett, S. Mitragotri, A. Yamamoto, R. Langer, and J. Weaver, "Synergistic effect of electric field and ultrasound on transdermal transport," *Pharmaceutical research*, vol. 13, no. 4, pp. 633–638, 1996.

[36] K. Fukushima, A. Ise, H. Morita, R. Hasegawa, Y. Ito, N. Sugioka, and K. Takada, "Two-layered dissolving microneedles for percutaneous delivery of peptide/protein drugs in rats," *Pharmaceutical research*, vol. 28, no. 1, pp. 7–21, 2011.

[37] M. B. Brown, M. J. Traynor, G. P. Martin, and F. K. Akomeah, "Transdermal drug delivery systems: skin perturbation devices," *Drug delivery systems*, pp. 119–139, 2008.

[38] H. Marwah, T. Garg, A. K. Goyal, and G. Rath, "Permeation enhancer strategies in transdermal drug delivery," *Drug delivery*, vol. 23, no. 2, pp. 564–578, 2016.

[39] G. Ma and C. Wu, "Microneedle, bio-microneedle and bio-inspired microneedle: A review," *Journal of Controlled Release*, vol. 251, pp. 11–23, 2017.

[40] S. Indermun, R. Luttge, Y. E. Choonara, P. Kumar, L. C. Du Toit, G. Modi, and V. Pillay, "Current advances in the fabrication of microneedles for transdermal delivery," *Journal of controlled release*, vol. 185, pp. 130–138, 2014.

[41] N. R. Hegde, S. V. Kaveri, and J. Bayry, "Recent advances in the administration of vaccines for infectious diseases: microneedles as painless delivery devices for mass vaccination," *Drug discovery today*, vol. 16, no. 23-24, pp. 1061–1068, 2011.

[42] M. R. Prausnitz, "Microneedles for transdermal drug delivery," *Advanced drug delivery reviews*, vol. 56, no. 5, pp. 581–587, 2004.

[43] M. Haq, E. Smith, D. N. John, M. Kalavala, C. Edwards, A. Anstey, A. Morrissey, and J. C. Birchall, "Clinical administration of microneedles: skin puncture, pain and sensation," *Biomedical microdevices*, vol. 11, no. 1, pp. 35–47, 2009.

[44] K. Van Der Maaden, W. Jiskoot, and J. Bouwstra, "Microneedle technologies for (trans) dermal drug and vaccine delivery," *Journal of controlled release*, vol. 161, no. 2, pp. 645–655, 2012.

[45] M. J. Kim, S. C. Park, B. Rizal, G. Guanes, S.-K. Baek, J.-H. Park, A. R. Betz, and S.-O. Choi, "Fabrication of circular obelisk-type multilayer microneedles using micro-milling and spray deposition," *Frontiers in bioengineering and biotechnology*, vol. 6, p. 54, 2018.

[46] B. Bediz, E. Korkmaz, R. Khilwani, C. Donahue, G. Erdos, L. D. Falo, and O. B. Ozdoganlar, "Dissolvable microneedle arrays for intradermal delivery of biologics: fabrication and application," *Pharmaceutical research*, vol. 31, no. 1, pp. 117–135, 2014.

[47] A. R. Johnson, C. L. Caudill, J. R. Tumbleston, C. J. Bloomquist, K. A. Moga, A. Ermoshkin, D. Shirvanyants, S. J. Mecham, J. C. Luft, and J. M. DeSimone, "Single-step fabrication of computationally designed microneedles by continuous liquid interface production," *PloS one*, vol. 11, no. 9, p. e0162518, 2016.

[48] S. C. Balmert, C. D. Carey, G. D. Falo, S. K. Sethi, G. Erdos, E. Korkmaz, and L. D. Falo Jr, "Dissolving undercut microneedle arrays for multicomponent cutaneous vaccination," *Journal of Controlled Release*, vol. 317, pp. 336–346, 2020.

[49] W.-G. Bae, H. Ko, J.-Y. So, H. Yi, C.-H. Lee, D.-H. Lee, Y. Ahn, S.-H. Lee, K. Lee, J. Jun, *et al.*, "Snake fang–inspired stamping patch for transdermal delivery of liquid formulations," *Science Translational Medicine*, vol. 11, no. 503, p. eaaw3329, 2019.

[50] Y.-C. Kim, J.-H. Park, and M. R. Prausnitz, "Microneedles for drug and vaccine delivery," *Advanced drug delivery reviews*, vol. 64, no. 14, pp. 1547–1568, 2012.

[51] D. F. Fonseca, C. Vilela, A. J. Silvestre, and C. S. Freire, "A compendium of current developments on polysaccharide and protein-based microneedles," *International journal of biological macromolecules*, vol. 136, pp. 704–728, 2019.

[52] J. W. Lee, S.-O. Choi, E. I. Felner, and M. R. Prausnitz, "Dissolving microneedle patch for transdermal delivery of human growth hormone," *Small*, vol. 7, no. 4, pp. 531–539, 2011.

[53] E. Korkmaz, S. C. Balmert, T. L. Sumpter, C. D. Carey, G. Erdos, and L. D. Falo Jr, "Microarray patches enable the development of skin-targeted vaccines against covid-19," *Advanced Drug Delivery Reviews*, vol. 171, pp. 164–186, 2021.

[54] R. S. Ingrole and H. S. Gill, "Microneedle coating methods: A review with a perspective," *Journal of Pharmacology and Experimental Therapeutics*, vol. 370, no. 3, pp. 555–569, 2019.

[55] A. J. Paredes, P. E. McKenna, I. K. Ramöller, Y. A. Naser, F. Volpe-Zanutto, M. Li, M. Abbate, L. Zhao, C. Zhang, J. M. Abu-Ershaid, *et al.*, "Microarray patches: poking a hole in the challenges faced when delivering poorly soluble drugs," *Advanced Functional Materials*, vol. 31, no. 1, p. 2005792, 2021.

[56] K. Vinayakumar, P. G. Kulkarni, M. Nayak, N. Dinesh, G. M. Hegde, S. Ramachandra, and K. Rajanna, "A hollow stainless steel microneedle array to deliver insulin to a diabetic rat," *Journal of Micromechanics and Microengineering*, vol. 26, no. 6, p. 065013, 2016.

[57] K. Ita, "Dissolving microneedles for transdermal drug delivery: Advances and challenges," *Biomedicine & Pharmacotherapy*, vol. 93, pp. 1116–1127, 2017.

[58] M. Leone, J. Mönkäre, J. A. Bouwstra, and G. Kersten, "Dissolving microneedle patches for dermal vaccination," *Pharmaceutical research*, vol. 34, no. 11, pp. 2223–2240, 2017.

[59] K. A. S. Al-Japairai, S. Mahmood, S. H. Almurisi, J. R. Venugopal, A. R. Hilles, M. Azmana, and S. Raman, "Current trends in polymer microneedle for transdermal drug delivery," *International journal of pharmaceutics*, vol. 587, p. 119673, 2020.

[60] P. R. Yadav, T. Han, O. Olatunji, S. K. Pattanayek, and D. B. Das, "Mathematical modelling, simulation and optimisation of microneedles for transdermal drug delivery: trends and progress," *Pharmaceutics*, vol. 12, no. 8, p. 693, 2020.

[61] B. Sabitha and N. Muniraj, "Structural analysis of hollow titanium microneedle for amniotic fluidic extraction," in *2013 International Conference on Optical Imaging Sensor and Security (ICOSS)*, pp. 1–5, IEEE, 2013.

[62] Z. Chen, Y. Lin, W. Lee, L. Ren, B. Liu, L. Liang, Z. Wang, and L. Jiang, "Additive manufacturing of honeybee-inspired microneedle for easy skin insertion and difficult removal," *ACS applied materials & interfaces*, vol. 10, no. 35, pp. 29338–29346, 2018.

[63] J. Brazzle, I. Papautsky, and A. B. Frazier, "Micromachined needle arrays for drug delivery or fluid extraction," *IEEE engineering in medicine and biology magazine*, vol. 18, no. 6, pp. 53–58, 1999.

[64] S. P. Davis, B. J. Landis, Z. H. Adams, M. G. Allen, and M. R. Prausnitz, "Insertion of microneedles into skin: measurement and prediction of insertion force and needle fracture force," *Journal of biomechanics*, vol. 37, no. 8, pp. 1155–1163, 2004.

[65] B. Al-Qallaf and D. B. Das, "Optimizing microneedle arrays to increase skin permeability for transdermal drug delivery," *Annals of the New York Academy of Sciences*, vol. 1161, no. 1, pp. 83–94, 2009.

[66] G. Yan, K. S. Warner, J. Zhang, S. Sharma, and B. K. Gale, "Evaluation needle length and density of microneedle arrays in the pretreatment of skin for transdermal drug delivery," *International journal of Pharmaceutics*, vol. 391, no. 1-2, pp. 7–12, 2010.

[67] J.-H. Oh, H.-H. Park, K.-Y. Do, M. Han, D.-H. Hyun, C.-G. Kim, C.-H. Kim, S. S. Lee, S.-J. Hwang, S.-C. Shin, *et al.*, "Influence of the delivery systems using a microneedle array on the permeation of a hydrophilic molecule, calcein," *European journal of pharmaceutics and biopharmaceutics*, vol. 69, no. 3, pp. 1040–1045, 2008.

[68] B. Stoeber and D. Liepmann, "Arrays of hollow out-of-plane microneedles for drug delivery," *Journal of Microelectromechanical systems*, vol. 14, no. 3, pp. 472–479, 2005.

[69] E. Z. Loizidou, N. A. Williams, D. A. Barrow, M. J. Eaton, J. McCrory, S. L. Evans, and C. J. Allender, "Structural characterisation and transdermal delivery studies on sugar microneedles: Experimental and finite element modelling analyses," *European Journal of Pharmaceutics and Biopharmaceutics*, vol. 89, pp. 224–231, 2015.

[70] R. Groves, "Quantifying the mechanical properties of skin in vivo and ex vivo to optimize microneedle device design," *Doctor in Biomechanics, Cardiff University*, 2011.

[71] D. W. Bodhale, A. Nisar, and N. Afzulpurkar, "Structural and microfluidic analysis of hollow side-open polymeric microneedles for transdermal drug delivery applications," *Microfluidics and Nanofluidics*, vol. 8, no. 3, pp. 373–392, 2010.

[72] R. K. Haldkar, V. K. Gupta, and T. Sheorey, "Modeling and flow analysis of piezoelectric based micropump with various shapes of microneedle," *Journal of Mechanical Science and Technology*, vol. 31, no. 6, pp. 2933–2941, 2017.

[73] O. Olatunji, D. B. Das, M. J. Garland, L. Belaid, and R. F. Donnelly, "Influence of array interspacing on the force required for successful microneedle skin penetration: theoretical and practical approaches," *Journal of pharmaceutical sciences*, vol. 102, no. 4, pp. 1209–1221, 2013.

[74] S. Aoyagi, H. Izumi, and M. Fukuda, "Biodegradable polymer needle with various tip angles and consideration on insertion mechanism of mosquito's

proboscis," *Sensors and Actuators A: Physical*, vol. 143, no. 1, pp. 20–28, 2008.

[75] X. Kong, P. Zhou, and C. Wu, "Numerical simulation of microneedles' insertion into skin," *Computer methods in biomechanics and biomedical engineering*, vol. 14, no. 9, pp. 827–835, 2011.

[76] M. R. Sarabi, B. Bediz, L. D. Falo, E. Korkmaz, and S. Tasoglu, "3d printing of microneedle arrays: challenges towards clinical translation," 2021.

[77] S. R. Dabbagh, M. R. Sarabi, R. Rahbarghazi, E. Sokullu, A. K. Yetisen, and S. Tasoglu, "3d-printed microneedles in biomedical applications," *Iscience*, vol. 24, no. 1, p. 102012, 2021.

[78] K. J. Krieger, N. Bertollo, M. Dangol, J. T. Sheridan, M. M. Lowery, and E. D. O'Cearbhaill, "Simple and customizable method for fabrication of high-aspect ratio microneedle molds using low-cost 3d printing," *Microsystems & nanoengineering*, vol. 5, no. 1, pp. 1–14, 2019.

[79] M. A. Luzuriaga, D. R. Berry, J. C. Reagan, R. A. Smaldone, and J. J. Gassensmith, "Biodegradable 3d printed polymer microneedles for transdermal drug delivery," *Lab on a Chip*, vol. 18, no. 8, pp. 1223–1230, 2018.

[80] J. R. Tumbleston, D. Shirvanyants, N. Ermoshkin, R. Janusziewicz, A. R. Johnson, D. Kelly, K. Chen, R. Pinschmidt, J. P. Rolland, A. Ermoshkin, *et al.*, "Continuous liquid interface production of 3d objects," *Science*, vol. 347, no. 6228, pp. 1349–1352, 2015.

[81] Z. F. Rad, P. D. Prewett, and G. J. Davies, "An overview of microneedle applications, materials, and fabrication methods," *Beilstein Journal of Nanotechnology*, vol. 12, no. 1, pp. 1034–1046, 2021.

[82] J. Yang, X. Liu, Y. Fu, and Y. Song, "Recent advances of microneedles for biomedical applications: drug delivery and beyond," *Acta Pharmaceutica Sinica B*, vol. 9, no. 3, pp. 469–483, 2019.

[83] H. Chang, M. Zheng, X. Yu, A. Than, R. Z. Seeni, R. Kang, J. Tian, D. P. Khanh, L. Liu, P. Chen, *et al.*, "A swellable microneedle patch to rapidly extract skin interstitial fluid for timely metabolic analysis," *Advanced Materials*, vol. 29, no. 37, p. 1702243, 2017.

[84] G. Fabbrocini, V. De Vita, A. Monfrecola, M. P. De Padova, B. Brazzini, F. Teixeira, and A. Chu, "Percutaneous collagen induction: an effective and safe treatment for post-acne scarring in different skin phototypes," *Journal of dermatological treatment*, vol. 25, no. 2, pp. 147–152, 2014.

[85] H. Huang, H. Xu, and J. Zhang, "Current tissue engineering approaches for cartilage regeneration," *Cartilage tissue engineering and regeneration techniques*, vol. 13, 2019.

[86] S. L. Kolasinski, T. Neogi, M. C. Hochberg, C. Oatis, G. Guyatt, J. Block, L. Callahan, C. Copenhaver, C. Dodge, D. Felson, *et al.*, "2019 american college of rheumatology/arthritis foundation guideline for the management of osteoarthritis of the hand, hip, and knee," *Arthritis & Rheumatology*, vol. 72, no. 2, pp. 220–233, 2020.

[87] M. Kanwischer, S.-Y. Kim, S. Bian, K. A. Kwon, J. S. Kim, and D.-D. Kim, "Evaluation of the physicochemical stability and skin permeation of glucosamine sulfate," *Drug development and industrial pharmacy*, vol. 31, no. 1, pp. 91–97, 2005.

[88] J. Jerosch, "Effects of glucosamine and chondroitin sulfate on cartilage metabolism in oa: outlook on other nutrient partners especially omega-3 fatty acids," *International journal of rheumatology*, vol. 2011, 2011.

[89] P. Khanna, K. Luongo, J. A. Strom, and S. Bhansali, "Sharpening of hollow silicon microneedles to reduce skin penetration force," *Journal of Micromechanics and Microengineering*, vol. 20, no. 4, p. 045011, 2010.

[90] E. Korkmaz, E. E. Friedrich, M. H. Ramadan, G. Erdos, A. R. Mathers, O. B. Ozdoganlar, N. R. Washburn, and L. D. Falo Jr, "Therapeutic intradermal delivery of tumor necrosis factor-alpha antibodies using tip-loaded dissolvable microneedle arrays," *Acta biomaterialia*, vol. 24, pp. 96–105, 2015.

[91] R. R. S. Thakur, I. A. Tekko, F. Al-Shammari, A. A. Ali, H. McCarthy, and R. F. Donnelly, "Rapidly dissolving polymeric microneedles for minimally invasive intraocular drug delivery," *Drug delivery and translational research*, vol. 6, no. 6, pp. 800–815, 2016.

[92] W. Sun, Z. Araci, M. Inayathullah, S. Manickam, X. Zhang, M. A. Bruce, M. P. Marinkovich, A. T. Lane, C. Milla, J. Rajadas, *et al.*, "Polyvinylpyrrolidone microneedles enable delivery of intact proteins for diagnostic and therapeutic applications," *Acta biomaterialia*, vol. 9, no. 8, pp. 7767–7774, 2013.

[93] S. N. Alconcel, A. S. Baas, and H. D. Maynard, "Fda-approved poly (ethylene glycol)–protein conjugate drugs," *Polymer Chemistry*, vol. 2, no. 7, pp. 1442–1448, 2011.

[94] M. Sarmadi, K. McHugh, R. Langer, and A. Jaklenec, "Multi-objective optimization of microneedle design for transdermal drug delivery," *Stress*, vol. 10, p. 15, 2019.

[95] S. J. Blank and M. F. Hutt, "Antenna array synthesis using derivative, nonderivative and random search optimization," in *2008 IEEE Sarnoff Symposium*, pp. 1–4, IEEE, 2008.

[96] A. Fast, "Nsga-ii," *Kanpur Genetic Algorithms Laboratory, India, Kangal Report*, no. 200001, 2000.

[97] S. Lotfan, R. A. Ghiasi, M. Fallah, and M. Sadeghi, "Ann-based modeling and reducing dual-fuel engine's challenging emissions by multi-objective evolutionary algorithm nsga-ii," *Applied energy*, vol. 175, pp. 91–99, 2016.

[98] T. Yalcinoz, H. Altun, and M. Uzam, "Economic dispatch solution using a genetic algorithm based on arithmetic crossover," in *2001 IEEE Porto Power Tech Proceedings (Cat. No. 01EX502)*, vol. 2, pp. 4–pp, IEEE, 2001.

[99] L. Xie, S. Brownridge, O. Ozdoganlar, and L. Weiss, "The viability of micromilling for manufacturing mechanical attachment components for medical applications," *Trans. NAMRI/SME*, vol. 34, pp. 445–452, 2006.

[100] M. P. Wolf, G. B. Salieb-Beugelaar, and P. Hunziker, "Pdms with designer functionalities—properties, modifications strategies, and applications," *Progress in Polymer Science*, vol. 83, pp. 97–134, 2018.

[101] K. D. Ngadimin, A. Stokes, P. Gentile, and A. M. Ferreira, "Biomimetic hydrogels designed for cartilage tissue engineering," *Biomaterials Science*, vol. 9, no. 12, pp. 4246–4259, 2021.

[102] J. S. Kochhar, W. J. Soon, J. Choi, S. Zou, L. Kang, *et al.*, "Effect of microneedle geometry and supporting substrate on microneedle array penetration into skin," *Journal of Pharmaceutical Sciences*, vol. 102, no. 11, pp. 4100–4108, 2013.

[103] A. Dąbrowska, G. M. Rotaru, F. Spano, C. Affolter, G. Fortunato, S. Lehmann, S. Derler, N. D. Spencer, and R. M. Rossi, "A water-responsive, gelatine-based human skin model," *Tribology International*, vol. 113, pp. 316–322, 2017.

[104] A. Adan, Y. Kiraz, and Y. Baran, "Cell proliferation and cytotoxicity assays," *Current pharmaceutical biotechnology*, vol. 17, no. 14, pp. 1213–1221, 2016.

[105] C.-C. Liang, A. Y. Park, and J.-L. Guan, "In vitro scratch assay: a convenient and inexpensive method for analysis of cell migration in vitro," *Nature protocols*, vol. 2, no. 2, pp. 329–333, 2007.

[106] A. Travan, F. Scognamiglio, M. Borgogna, E. Marsich, I. Donati, L. Tarusha, M. Grassi, and S. Paoletti, "Hyaluronan delivery by polymer demixing in polysaccharide-based hydrogels and membranes for biomedical applications," *Carbohydrate polymers*, vol. 150, pp. 408–418, 2016.